

Review

A Review on Solar Chimneys: From Natural Convection Fundamentals to Thermohydraulic Best-Performance Proposals

Blas Zamora 

Department of Thermal and Fluids Engineering, Technical University of Cartagena, 30202 Cartagena, Spain; blas.zamora@upct.es

Abstract: This work presents an overview of (passive) solar chimney research, from the natural convection fundamentals to the recent progress for achieving thermohydraulic best-performance. Solar chimneys are attractive because they contribute to increasing the efficiency in air conditioning processes for dwellings and buildings, and therefore also aid to reduction in greenhouse gas emissions. A wide number of works dealing with solar chimneys (and Trombe walls or similar) shape designs, as well as with the inclusion of obstacles for disturbing the airflow, is commented in detail. Several numerical simulation procedures used in the literature are specially discussed, and different recommendations are pointed out to be considered for the appropriate numerical simulation of the operating modes of a solar chimney. Investigations aiming for the best performance conditions (for both thermal, and dynamic or ventilation modes) deserve special attention.

Keywords: passive solar design; solar chimney; Trombe wall; best-performance behavior; natural ventilation; heat transfer enhancement; numerical modeling

1. Introduction

1.1. Fundamentals of Natural Convection Flows

The main objective of this technical literature review is to provide researchers and professionals with a global vision of the methods for studying passive thermal systems used in the air conditioning of buildings. The review conducted may differ slightly from many of those reported in which the classification of published works has often been prioritized based on certain aspects related to the focus of research. In this paper, the discussion starts from the physical basis of flows induced by natural convection, and its application to the fundamental problem of flows established in parallel plate and wall systems; the focus is mainly on solar chimneys and specifically in their shape designs, as well as in the introduction of obstacles and turbulence or vortex generators. Therefore, it can be deduced from the above that focus is posed on the analysis and simulation (especially the *numerical simulation*) of the established airflows, and on their repercussions on the design of passive solar systems: optimization of the wall-to-wall distances, parametric analysis of shapes and designs, and more.

It is noteworthy that denomination *solar chimney* or *thermal chimney* usually refers to both passive thermal devices (without power mechanisms) and plants with electricity generation. The latter can be distinguished as *solar tower* or *solar chimney (power) plant*, or similar. The scope of the present work is concerned to the former, i.e., attention is posed on fully passive solar chimneys.

Heat transfer by *convection* is produced by the mixing of different parts of the fluid due to mass motions. The dynamic characteristics of the flow (for example, the velocity or the turbulence intensity fields) strongly influence, for example, the heat transferred between the fluid and a given wall. The motion of the fluid can be originated by external mechanical causes such as the existence of a fan or a pump, being the process known as *forced convection*, or by density differences created by temperature gradients that exist in the



Citation: Zamora, B. A Review on Solar Chimneys: From Natural Convection Fundamentals to Thermohydraulic Best-Performance Proposals. *Processes* **2023**, *11*, 386. <https://doi.org/10.3390/pr11020386>

Academic Editors: Kian Jon Chua and Iztok Golobič

Received: 1 December 2022

Revised: 24 January 2023

Accepted: 24 January 2023

Published: 27 January 2023



Copyright: © 2023 by the author. Licensee MDPI, Basel, Switzerland. This article is an open access article distributed under the terms and conditions of the Creative Commons Attribution (CC BY) license (<https://creativecommons.org/licenses/by/4.0/>).

mass of the fluid (*buoyancy forces*), being known as *natural convection* (Bejan [1], Incropera and De Witt [2], Bejan [3]).

In *natural (or free) convection*, the motion of the fluid is induced by buoyancy forces. These forces are concerned with the general trends of fluids to expand when they are heated at constant pressure (Turner [4]). In engineering applications involving natural convection the target may be to determine the heat transfer coefficient between the solid and the fluid (in order to know the total heat flux transferred), or alternately to calculate the induced mass-flow rate through a given section.

It is well known that heat transfer due to natural convection is low compared to that by forced convection for equivalent situations. However, natural convection is a very attractive heat transfer mode in cases in which ease of construction, economy, or low noise are design requirements. For example, in the case of cooling electronic equipment, passive thermal control continues to be preferred due to their low cost and maintenance and because these systems do not cause electromagnetic interferences. Another relevant application is the emergency cooling systems of nuclear reactors. Here, liquid metals acting as coolants can be found in fast breeder reactors after a severe accident. Liquid sodium and liquid gallium are the most employed liquid metals, because of their notoriously low *Prandtl number* ($Pr = \nu/\alpha$, being ν the kinematic viscosity and α the thermal diffusivity). However, as will be seen later in more detail, the fundamental applications that are the subject of this review are the passive thermal systems dedicated to natural ventilation, or passive heating or cooling, in systems and structures such as dwellings or buildings.

Since the applications are very diverse, different typical configurations have been studied so far such as cavities or enclosures (partially open or closed), or vertical channel systems. Regardless of the configuration under consideration, the presence of heated walls encourages the natural generation of fluid flow. The most used fluid is air ($Pr \approx 0.7$), and to a lesser extent water ($Pr \approx 7$). From now on, attention is posed on air.

The *relevant parameters* to be considered are based on the height of the heated wall H (Figure 1) and on the characteristic temperature difference $\Delta T = T_w - T_\infty$, being T_w and T_∞ the wall and ambient temperatures, respectively. Hence, the Grashof (Gr_H) and Rayleigh (Ra_H) numbers are, respectively, defined as:

$$Gr_H = \frac{g\beta(\Delta T)H^3}{\nu^2}, \quad Ra_H = Gr_H Pr \quad (1)$$

with g the gravity acceleration and the volumetric expansion coefficient $\beta = 1/T_\infty$ (perfect gas assumption for air). Therefore, the heat transfer coefficient can be evaluated through the *average Nusselt number* (Nu_H) at the heated wall. If the wall can be considered isothermal, Nusselt number is calculated as follows:

$$Nu_H = - \int_H \frac{(\partial T/\partial x)_w}{T_w - T_\infty} dy \quad (2)$$

in which w denotes solid wall and y the direction along the wall (Figure 1). In general, flows induced by natural convection phenomena have low velocities, so that on many occasions the established flow can be considered *laminar*. However, under given circumstances, the flow can be transitional or even fully *turbulent*. This occurs in a great number of passive thermal systems in which the large scale of geometrical dimensions could produce high turbulence levels. Usually, the criterion employed is based on the Grashof number with the transition taking place for values of this parameter roughly above 10^9 .

1.2. Turbulence and Numerical Simulations

As expected, natural convection airflows have been extensively studied analytically, experimentally, and numerically. Following, some topics on the simulation methods are treated, particularly for a turbulent regime. In general, the most widely used treatment by commercial *Computational Fluid Dynamics* (CFD) codes is the numerical solution of the *Reynolds Averaged Navier–Stokes* (RANS) equations.

An appropriate form of the RANS equations for the problem (continuity, momentum and energy), using the *Boussinesq approximation* (which will be explained later) for the buoyancy term, is listed following (x_j denotes Cartesian coordinates and t the time):

$$\frac{\partial \rho}{\partial t} = -\frac{\partial(\rho U_j)}{\partial x_j} \quad (3)$$

$$\frac{\partial(\rho U_i)}{\partial t} + \frac{\partial(\rho U_i U_j)}{\partial x_j} = -\frac{\partial P}{\partial x_i} + \frac{\partial}{\partial x_j} \left(\mu \frac{\partial U_i}{\partial x_j} - \rho \overline{u_i u_j} \right) + \rho g_i \beta (T - T_\infty) \quad (4)$$

$$\frac{\partial(\rho T)}{\partial t} + \frac{\partial(\rho c_p T U_j)}{\partial x_j} = \frac{\partial}{\partial x_j} \left(\kappa \frac{\partial T}{\partial x_j} - \rho c_p \overline{T' u_j} \right) \quad (5)$$

where T , P and U_j are the average temperature, the difference between the average pressure and the ambient pressure, and the average velocity, respectively. The alternating (turbulent) velocity is denoted as u_j . The Reynolds stress tensor $-\rho \overline{u_i u_j}$ and the heat flux vector $-\rho c_p \overline{T' u_j}$ should be supplied for an appropriate *turbulence model*. The thermal conductivity of fluid is κ ; ρ and μ are the density and (dynamic) viscosity, respectively, and c_p the specific heat at constant pressure. The gravity is $g_i = g$ in a vertical direction.

In CFD simulations turbulent two-transport equations models along with wall functions have been usually applied in problems including forced convection boundary layers for calculating the velocity and temperature gradients adjacent to walls. However, typical logarithmic wall functions do not seem to be appropriate in cases with natural convection boundary layers. Yuan et al. [5], among others, proposed new wall functions for numeric simulations of turbulent convective flows. Versteegh and Nieuwstadt [6] have studied the scaling behavior of natural convection flows to propose wall functions for flows established in vertical heated walls. On the basis on a matching of inner and outer layer scaling relationships, an explicit expression for the mean profile in the matching region was presented by these authors. On the other hand, Henkes and Hoogendorn [7] have analyzed turbulent convection in enclosures, explaining the difficulties found by using some turbulence models in order to predict correctly the heat transfer coefficients.

A literature survey seems to indicate that it can be appropriate to use standard models such as the $k-\varepsilon$ (k is the turbulent kinetic energy, and ε its dissipation rate), but taking into account the range of Grashof numbers for applying low-Reynolds (low-Re) number treatment at walls if necessary (Fedorov and Viskanta [8]). In a considerable number of works the $k-\omega$ (ω is the specific dissipation rate of ε) turbulence model of Kolmogorov (Wilcox [9]) and variants have been employed successfully. Hence, Peng and Davison [10] used the $k-\omega$ model for describing the turbulent flow generated by natural convection within a cavity. The low-Re treatment necessarily implies that some points of the grid must be immersed in the laminar sub-layer adjacent to walls. The degree of refinement of the mesh near the walls can be evaluated through the dimensionless sub-layer scaled distance, $y^+ = \rho y_1 u_\tau / \mu$, being y_1 the distance between the solid boundary and the first grid point, and u_τ the total friction velocity corresponding to wall shear stress τ_w ($u_\tau = [\tau_w / \rho]^{1/2}$). It is widely accepted that y^+ should be less than unity for achieving successful results. This limit is particularly relevant in the airflows established in solar passive systems in which laminar, transitional and fully turbulent flows can be identified.

The use of more complex models not based in the *eddy viscosity* concept (like those related to $k-\varepsilon$ or $k-\omega$ models) is also extended in technical literature, looking for a more physical detailed analysis of the buoyancy flows. For instance, Xu et al. [11] studied the problem of turbulence generated by buoyancy in a channel through a turbulence model which uses *Direct Numerical Simulation* (DNS) in the region close to the wall, and in turn the $k-\varepsilon$ model for the region away from the wall. From the results obtained through DNS techniques, Versteegh and Nieuwstadt [6] concluded that although natural convection (in vertical channels) could seem simple in terms of flow geometry, its physics as well as

its scaling behavior are far from simple. The latest trends seem to indicate that the *Large Eddy Simulation* (LES) models are being frequently employed (Ciofalo [12], Salinas-Vazquez et al. [13], among others).

A different manner to address the problem is that based on the *Lattice Boltzmann Methods* (LBM), a particular type of CFD procedure. Instead of solving a form of the Navier–Stokes equations directly, a given fluid density on a lattice is simulated with several processes such as streaming and collision between particles, achieving an approximation to fluid behavior. The method is versatile, but mathematically complex. Although a considerable number of works on thermal aspects can be found in the literature (Zhou et al. [14], among others), it can be stated that the use of LBM is not entirely generalized for the study of solar chimneys or Trombe walls, although LBM is frequently employed for other complex physical problems concerned to the matter (see the review of Nokhosteen and Sobhansarbandi [15]).

Obviously, although these advanced CFD techniques can achieve a more precise description of the flow, they require higher computational efforts. Two-dimensional simulations are frequently considered for computational effort saving. However, under given circumstances the morphology can force the address of the three-dimensional simulations. Even in cases with a clear 2D geometry, it is possible to find discrepancies in properties' distributions at different planes. However, in many cases 2D results could be extrapolated to 3D cases, subject to an appropriate morphological analysis.

1.3. Boussinesq Approach and Variable Properties

For the simulation of buoyancy forces the *Boussinesq* (or *Boussinesq–Oberbeck*) approach has been usually adopted. This approximation assumes the properties of fluid are constant, being the buoyancy force linearly due to temperature increases only, $\rho g \beta (T - T_\infty)$. In cases in which the temperature differences are relatively low the thermophysical properties of fluid can be assumed constant, and the Boussinesq approximation can be employed for the buoyancy term in the vertical component of momentum equation. Applications such as passive cooling in electronic equipment and intense heating conditions can be found in some cases. This can severely alter the properties of air, and therefore change previous predictions of the characteristic of airflow such as heat transfer and the mass-flow rate. Gray and Giorgini [16] studied the conditions of validity of the Boussinesq approach. Zhong et al. [17], and Emery and Lee [18] analyzed the effects of property variations on convective flows in a square enclosure. Chenoweth and Paolucci [19] demonstrated that the Boussinesq approach could produce significant errors for $(T - T_\infty) > 0.2T_\infty$.

When the effects of variation in the air thermophysical properties are retained, buoyancy force should be calculated directly from density gradients, $g(\rho_\infty - \rho)$. A contrasted result from researchers is that heat transfer coefficients and the induced mass-flow rate are considerably lower than those obtained assuming constant properties and the Boussinesq approach. This phenomenon can be attributed to the increase in the air viscosity (*viscous drag*), as well as the decrease in the air density that produces an additional thermally induced pressure drop (*thermal drag*) when the temperature difference increases (the phenomenon has been described by) Guo and Wu [20] and Guo et al. [21]. Summarily, both the thermal drag and the viscous drag increase faster than the buoyancy force as temperature increases. In addition, the flow patterns could be influenced strongly by the fluid variable properties for intense heating conditions. Note that this effect could be important in selected applications of solar passive systems.

1.4. Research Methodology and Scope

Several principles have been considered to carry out the work:

- Reviewing in comprehensive databases, such as scholar.google.com, sciencedirect.com, onlinelibrary.wiley.com, mdpi.com, springer.com, . . . , among others;
- Searching sufficient general keywords: natural convection, channels, solar chimneys, Trombe walls, buildings, ventilation;

- Selecting relevant published works. It has been preferred that the number of references not be too high, with the aim of conducting appropriate critical comments for most contributions;
- Focusing on solar chimneys in buildings, including Trombe walls;
- Focusing on certain aspects of the numerical simulations carried out, such as the use of turbulence models or the simulation of atmospheric wind, among others.

Regarding the scope of this manuscript, the main difference between the present review and other reported studies is the focus on the fundamentals of problem (Section 2) for addressing multiple aspects oriented to the best performance conditions. Section 3 is dedicated to vertical channels including extensions and different geometries, whereas in Section 4 attention is posed on geometries approximating passive solar devices. Sections 5–8 are focused on several solar chimney morphologies (and to a lesser extent in Trombe walls). Section 9 is a note on the effects of climate conditions, and finally Section 10 is a summary of the main proposed discussions and suggestions.

2. Basis: Vertical Channels

2.1. Fundamentals on Natural Convection in Vertical Channels

The solution of a natural convection problem has a purely physical interest attending that the change in momentum is coupled to the conservation of energy through buoyancy forces. As indicated, the motion of the fluid is not induced by the displacement of a boundary condition but by the generation of buoyancy forces within the fluid. In this sense, the orientation of the heated or cooled boundaries can be diverse, but it should be noted that the most efficient flows for engineering applications take place probably when walls are vertical.

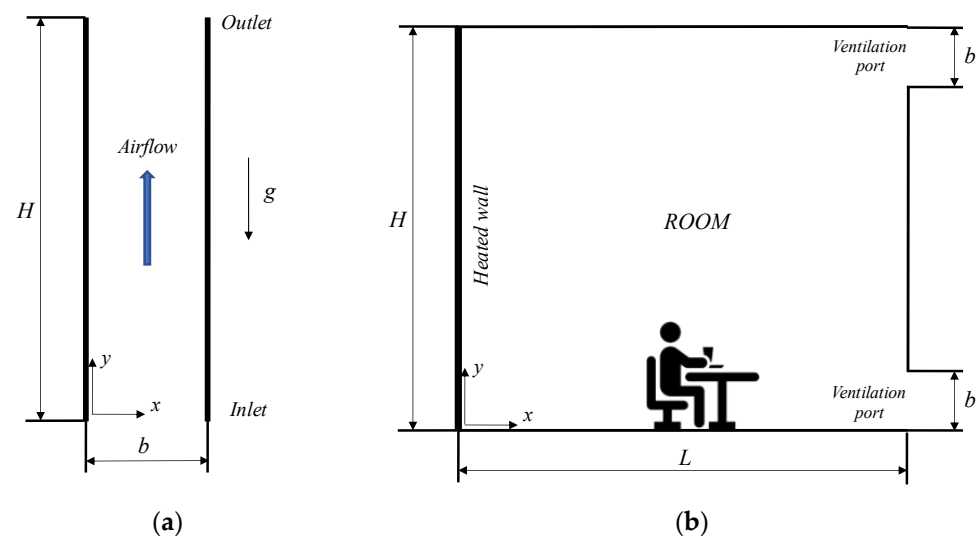


Figure 1. Basic configurations: (a) Simple vertical channel. Different symmetrical and asymmetrical heating conditions have been studied; (b) Typical arrangement of a cavity oriented to passive solar devices. Multiple combinations of heating conditions, and locations of apertures and ventilation ports have been analyzed in the literature.

Natural convection in vertical walls or plate systems has been the subject of intense study in recent years. A pioneering experimental study was carried out by Elenbaas [22] in vertical channels under uniform temperature at walls, considering laminar flow. Denoting b as the wall-to-wall distance of the channel and H as the height of heated walls (see Figure 1a), Elenbaas [22] proposed a correlation for the average Nusselt number (based on b) as a function of the modified Rayleigh number, $Ra_b^* = (Ra_b)(b/H)$, also based on b , which introduces the asymptotes for *boundary layer*, bl ($Nu_{bl} = 0.6(Ra_b^*)^{1/4}$, for $Ra_b^* \rightarrow \infty$), and for *fully developed*, fd ($Nu_{fd} = Ra_b^*/24$, for $Ra_b^* \rightarrow 0$) regimes. Aihara [23] was the first author who included the

pressure defect due to acceleration of fluid at the channel inlet. The numerical results were obtained through a line-by-line, forward marching, implicit finite-difference procedure, also for laminar regime. In fact, in the literature the first numerical results were obtained through the *finite-difference* discretization method and solving a *parabolic* form of the conservation equations. However, the nature of the flow is clearly *elliptic* irrespective of the fact that motion can be regarded as parabolic for asymptotic values of the relevant parameters, Grashof number or Rayleigh number. Kettleborough [24] and Nakamura et al. [25] reported the first numerical solutions of the elliptic form of the Navier–Stokes equations. More recently, a relevant review of benchmark solutions for flows induced by natural convection in vertical channels has been presented by Desrayaud et al. [26]. Wong and Chu [27] have reported a revisit on natural convection airflows from vertical isothermal plates; they developed a survey on the pioneer results presented for the thermally optimum plate spacing and have conducted own numerical computations.

2.2. The Optimization Problem

The optimization problem for systems formed by vertical plates can be represented by the electronic equipment cooling. Here, dissipating the heat generated in devices is important for avoid overheating. *Thermal optimization* of the problem can be achieved through the determination of the thermally optimum spacing, b_{opt} , between the plates or walls forming the vertical channels, which maximizes the heat transferred by unit area. Bodoia and Osterle [28] have given the first criterion for obtaining b_{opt} . Bar-Cohen and Rohsenow [29] proposed a blended-type correlation for the average Nusselt number (based on the fully developed and the boundary layer asymptotes) for obtaining the global heat transfer between the walls and the fluid. In this way, the optimum wall-to-wall distance is obtained for a given value of Ra_b^* , corresponding to cross area between the two mentioned asymptotes. Anand et al. [30] reported numerical results for the problem with different heating conditions at walls, and compared their results to those proposed by Bar-Cohen and Rohsenow [29].

Zamora and Hernández [31], similarly to Bar-Cohen and Rohsenow [29], used different correlations for the average Nusselt number to achieve thermal optimization. Values of b_{opt} were reached for a modified Rayleigh number Ra_b^* also placed near the crossing between the fully developed and the boundary layer asymptotes; thus, values of the optimum wall-to-wall distance depend on the fitting constants used in the correlations proposed for the average Nusselt number.

In view of the survey carried out two reasonings can be made. The first is that the cited numerical works simulate the flow as *laminar*. Obviously, depending mainly on the geometric scale of the physical application, the flow should be considered turbulent for relevant occasions. From now on, relevant works considering the turbulence of the flow will appear in the review. The second consists of the fact that considering configurations formed by (in general) isothermal vertical channel to obtain the optimal spacing between walls has physical sense if this morphology is regarded as a sample of the channels formed with equally spaced walls (usually at uniform temperature), located into a given horizontal length L . Let us consider that the number of plates or walls increases; thus, the total area available for heat transmission increases, but in turn the temperature gradient at walls tends to decrease, as well as the average heat transfer coefficient. The described effects reveal opposite when the number of plates decreases, then a thermally optimum wall-to-wall distance can be encountered. Consequently, if the *theoretical* b_{opt} is $b_{opt} > L$, only one channel can be formed into the available space. Although the global heat transfer is probably not maximum in this case, its value will be higher than that reached by mounting more than one channel.

Looking for morphologies of application in passive thermal systems (for buildings), Zamora [32] has determined numerically the thermally optimum spacing between inner isothermal plates into a vented cavity. From numerical results, a practical correlation for the optimum aspect ratio of inner channel is provided as a function of Rayleigh number,

and valid for laminar/turbulent flow. The influence of variable thermophysical properties has been taken into account through a heating parameter given by $\Delta T/T_\infty$. Results have been obtained by means of a finite volume procedure with the CFD general-purpose code Phoenix (provided by pioneering CHAM).

3. Vertical Channels with Extensions

3.1. Additional Spaces in Vertical Channels Systems

Effects of additional spaces on the behavior or systems of vertical channels are also analyzed in the literature. One of the first works dealing with a systematic study on the *chimney effect* (pioneeringly treated by Haaland and Sparrow [33]) in the enhancement of heat transfer in isothermal channels was that of Straatman et al. [34], both experimentally (by means of Mach-Zehnder interferometer) and numerically. The chimney effect is based on the idea that for enhancing the heat transfer in simple vertical structures more account of fluid must be forced through the system so that additional energy can be convected out. This can be achieved with the inclusion of adiabatic extensions, for instance. Straatman et al. [34] encountered heat transfer enhancements between 1.1 and 1.3. Morrone et al. [35] addressed a similar study but considered an I-shaped computational domain including two large rectangular reservoirs at the entrance and the exit of the channel, in which plates were asymmetrically heated by uniform heat flux. Ledezma and Bejan [36] numerically addressed the optimal geometric arrangement of staggered vertical plates in laminar regime, through the *method of intersection of asymptotes*. Numerical results were obtained by means of a commercial code based on the weighted residuals method of Galerkin. A similar numerical method was employed by Viswamula and Ruhul Amin [37] for addressing the effects of multiple obstructions on the thermal behavior of an isothermal vertical channel. They found that obstructions produce maximum reduction in heat transfer approximately equal to 30% compared to unobstructed channel. The presence of elements such as fins, usually used to improve the thermal behavior of forced convection systems, often has an obstructive effect on systems in which the motion is induced by buoyancy forces. Therefore, depending on the flow regime, laminar, transitional, or turbulent, and the geometry considered, the effect could be favorable or unfavorable. Zhang and Liu [38] found a significant increase in the transferred heat flux for vertical rectangular fin arrays, compared to un-finned ones. They carried out numerical calculations for investigating the influence of both the fin thickness and the spacing between fins. Note that in this case fins do not have an obstructive effect; in turn, they are placed along the mainstream of the fluid. We will return to this matter later.

Keep in mind that in general, turbulent flow is more efficient than laminar flow for engineering applications (for a vertical isolated wall, $Nu_H \approx Ra_H^{1/4}$ for laminar flow, whereas $Nu_H \approx Ra_H^{1/3}$ for turbulent flow). For this reason, the introduction of turbulence generators is another element that has been studied for achieving improvement in the thermal behavior of these systems (Ben Maad and Belghith [39]). Fedorov and Viskanta [8] probed that the increase in turbulence intensity at the entrance of channels drives to obtain higher heat transfer coefficients at walls, both experimentally and numerically.

3.2. Note on Optimization Procedures

Different procedures for determining best performance conditions have been utilized, from the usual *parametric analysis* to the *scale analysis* (or order-of-magnitude) method, as well as the *intersection of the asymptotes* corresponding to different regimes of the flow. The last is similar to that addressed by Bar-Cohen and Rohsenow [29] and Zamora and Hernández [33]. Another feasible method is based on the *Constructal Law* of Bejan (Bejan [40], Bejan and Lorente [41]). These authors pointed out that the basis of the constructal theory is formed by the *global objectives* and the *global constraints*, providing universality. The more relevant point is that the geometry of the flow is unknown, i.e., the geometry is not previously assumed, and in turn it should be deduced. This fact makes the procedure especially attractive although it obviously has some complexity and could be laborious.

For instance, da Silva et al. [42] used the constructal method to determine the optimal distribution and sizes of discrete heat sources in a vertical channel. They considered two types of geometry: firstly, heat sources with fixed size and fixed heat flux; and secondly, single heat source with variable size and fixed total heat flux.

4. Geometries Approximating Passive Solar Devices

4.1. Some Topics on Studied Morphologies

Enclosures or cavities (see Figure 1b) have been considered as typical arrangements to approximate studies to practical situations [7,10,13,32]. Configurations considered, for instance, by da Silva and Gosselin [43] are undoubtedly already applicable to passive thermal systems. They carried out numerical simulations for obtaining the optimal geometry of L- and C-shaped channels for maximum heat transfer in laminar natural convection. Global constraint was the total height H of the channel. The values of the obtained optimal spacing decrease as Ra_H increases for Ra_H in the range 10^5 – 10^7 . They also employed the intersection of asymptotes method. Zamora and Kaiser [44] carried out massive computations through the CFD Phoenics code for obtaining the optimum wall-to-wall spacing in an L-shaped channel with solar chimney geometry. The considered wide range of Rayleigh numbers covered the laminar, transitional and turbulent regimes. Values obtained for the *optimum* (*opt*) aspect ratio $(b/H)_{opt}$ maximizing the heat transfer were less than those maximizing the induced mass-flow rate m (kg/s). They provided correlations of $(b/H)_{opt}$ for isothermal heating conditions as a function of Rayleigh number. Turbulent simulations were obtained through the k – ω turbulence model of Wilcox [9]. These authors extended their study to a C-shaped channel simulating a truncated Trombe wall geometry (Zamora and Kaiser [45]) and presented correlations for the aspect ratio $(b/H)_{opt}$ that respectively maximized the heat transfer between the fluid and the walls, and the induced mass-flow rate, for symmetrically isothermal heating conditions. Similar to the trend obtained by da Silva and Gosselin [43], the higher the value of Ra_H , the lower the value of $(b/H)_{opt}$. In addition, they pointed out that it was not feasible to optimize simultaneously both the dynamic and the thermal performance, although a certain energy function can be defined in order to find the global better performance of each system. In some cases (obviously in passive ventilation systems) the *dynamic optimization* is clearly interesting. Here, obtaining the maximum induced mass-flow rate m can become the target for ventilation purposes.

Like other authors, Zamora and Kaiser [44,45] also considered walls heated with a constant heat flux q (W/m^2), in which case Grashof number can be defined as:

$$Gr_H = \frac{g\beta q H^4}{\nu^2 \kappa} \quad (6)$$

Therefore, the *average Nusselt number* at the heated wall can be calculated as follows:

$$Nu_H = \frac{qH}{T_w - T_\infty} \quad (7)$$

where wall temperature T_w is not uniform along its surface; maximum value is reached in some intermediate point of the wall near the top. In this case, characteristic temperature could be the maximum value reached, or the average value at the wall, for instance. Behavior of the flow is clearly different when heating condition at the wall changes, and the existence of optimal values of the spacing between walls is at least debatable for heating conditions with heat flux at the walls. Most authors cited in this section have obtained values of the optimum gap only for isothermal conditions at walls. Irrespective of this fact, the physical reasoning for the existence of the optimum is still based on the opposite behavior achieved by the flow for the asymptotic limits that can be observed for different values of the parameters governing the system. The change in the relative size of the additional zones (inlet, outlet extensions) can influence the existence or not of the

maximum, as well as its values (if they exist), although to a lesser extent. Depending on the geometry the influence of eventual chimney effects could be relevant.

Other aspects of the matter can be treated and more realistic morphologies, alternative to channel systems, can be considered for obtaining more applied results. As expected, several works dealing with the geometric optimization of *cavity configurations* in order to obtaining the maximum heat transfer can be found in the literature (Aounallah et al. [46] for cavities with walls defined by Bezier curves; Biserni et al. [47] for H-shaped cavities; Lorenzini et al. [48] for T-shaped cavities, and Lorenzini and Rocha [49] for T-Y-shaped cavities, for instance).

4.2. Reference Studies on Passive Solar Systems

4.2.1. General Approach of Reference Studies

Solar collectors, thermosiphons, solar chimneys or Trombe walls are the best known devices used in the bioclimatic architecture. These thermal passive devices can help to reduce the electrical consumption in dwellings or buildings and are therefore included in the actual energy-sustainable strategies. Through a passive solar heating these structures are employed for achieving heating, cooling and ventilation in rooms and buildings. Focusing on solar chimneys (Figure 2) and Trombe walls (Figure 3), the device is often formed by a glazing receiving the irradiation, facing a massive wall (of concrete or masonry, usually), probably oriented to the south.

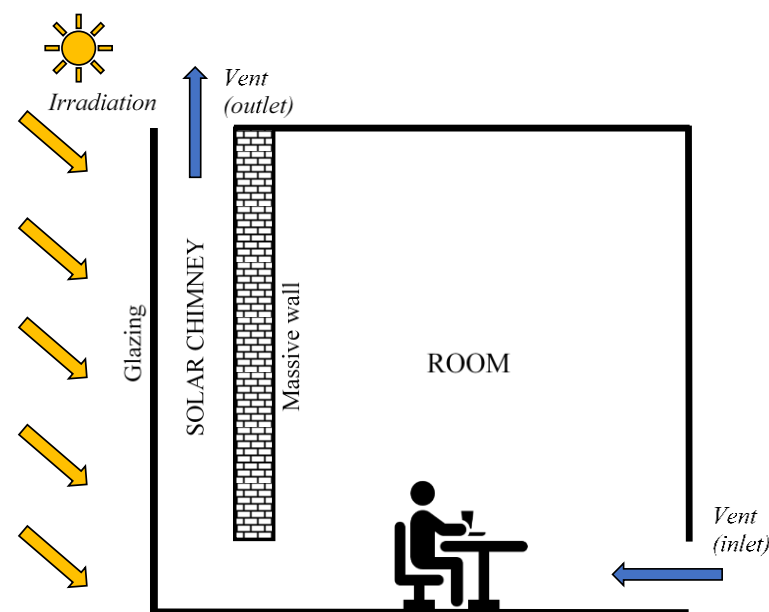


Figure 2. Typical arrangement of a solar chimney for natural ventilation and/or heating, attached to a room. Irradiation is captured through a special-purpose wall system (massive wall with absorber surface, glazing, . . .), forming a *channel*, or *cavity*, or *chimney* . . .

In Trombe walls (Figure 3) the massive wall acts as an energy storage from which the absorbed heat is emitted to the solar cavity or to the inside building. Vents are arranged in such a way that by opening or closing them different behavior modes can be achieved. In the winter, with heating mode, fresh air (or room air) enters through a vent located at the bottom of device, towards the space between the glazing and the wall (solar cavity, solar channel, solar chimney, etc.); here, air is heated and can enter the living room through an upper vent. This warm air produces natural heating for the building. In turn, in the summer, air enters at the bottom of the device from the inside room and is expelled to the outside due to the buoyancy forces, which produces a cooling of the interior of the room because of the induced natural ventilation.

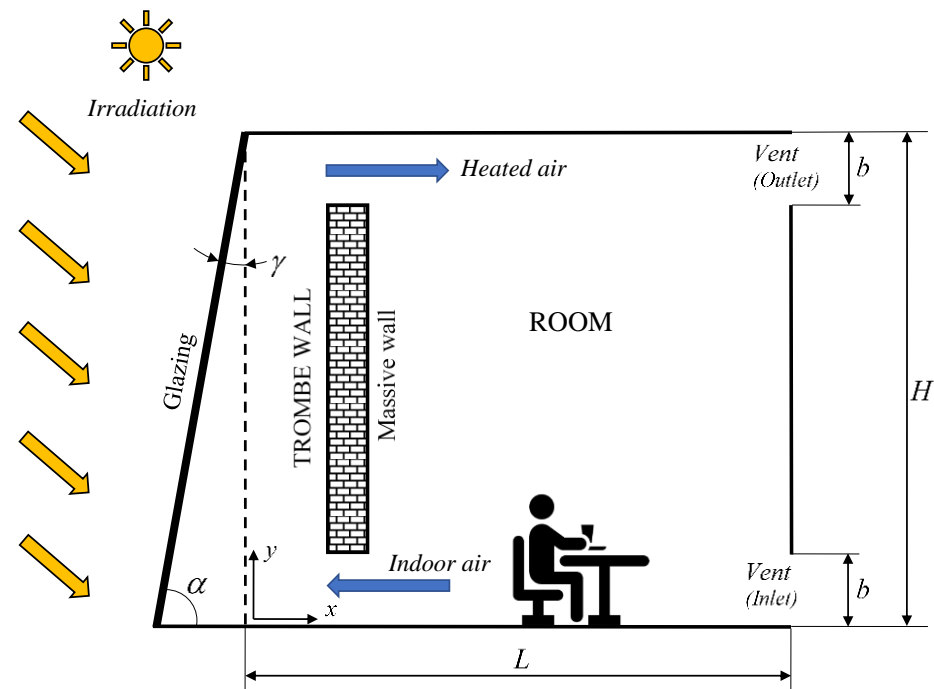


Figure 3. Typical arrangement of a Trombe wall attached to a room. The vents and apertures are placed to produce heating of indoor air (winter heating mode in the scheme). The thermally active walls (mainly the glazing) can be inclined (α or γ angles).

In solar chimneys (Figure 2) the main purpose is usually natural ventilation. Therefore, the solar chimney can consist of a solar collector formed by two walls attached to a room. The air enters through the bottom from the inside room and goes out through the open top, thus achieving a natural extraction of the air inside the building. However, glazing is also employed for obtaining higher irradiation capture. Therefore, it can be considered that a solar chimney is a particular case of Trombe wall. Depending on the morphological details and the opening or closing of given openings, different modes of operation can be achieved.

The fluid mechanics of natural ventilation were described in detail by Linden [50]. In general, the airflow can be generated both for temperature differences and for the wind. In fact, wind can become the dominant driving mechanism (*wind-driven* ventilation) but the *stack-driven* (or *buoyancy-driven*) ventilation is also important under given circumstances, and both mechanisms deserve especial attention. This author pointed out that several complex effects can appear, such as time-dependent flows, multiply connected spaces, non-adiabatic walls, or plume interactions, for instance.

4.2.2. Pioneering Works on Solar Passive Systems

Following on, several pioneering works on solar chimneys and Trombe walls are revised. Borgers and Akbari [51] reported a numerical study on the flow within a Trombe wall channel, using a mixing length model with empirical parameters considered in the literature for simulating the turbulence. Smolec and Thomas [52] explained that discrepancies encountered in heat transfer studies in Trombe walls could be due to oversimplified assumptions (such as uniform temperature at walls, and others). They carried out a review of typical engineering correlations to analytically describe the behavior of the passive solar system. The conventional model was extended to two-dimensional treatment (Smolec and Thomas [53]); the results were validated with experimental data.

Jubran et al. [54] presented numerical solutions for the laminar airflow in a Trombe wall, by means of a finite difference method. They considered a sloping glass wall. A given uniform vertical velocity was assumed as the entrance boundary condition in the computations. They concluded that increasing the tilt angle of glazing gave better performance

compared to the conventional vertical parallel channel, if tilt angles were kept small. Gan and Riffat [55] carried out a numerical study of solar chimneys including heat recovery; they concluded that installing heat pipes for heat recovery decreases the buoyancy force, and consequently reduces the ventilation capacity; additionally, the pressure loss increases. Note that this finding agrees with those obtained by other authors regarding the presence of obstacles into the fluid flow; in fact, Gan and Riffat [55] postulated that the most effective measure to increase the induced flow is to take advantage of the suction effect of the wind, if possible. Gan [56] presented a parametric study by numerical investigation using the *Renormalization Group* (RNG) $k-\epsilon$ turbulence model in enclosures with Trombe wall geometry. They concluded that in summer cooling mode the ventilation rate produced by natural convection increased with the wall temperature, as well as the height and the thickness of the heated wall.

Note that most investigations deal with airflows induced only by natural convection forces. Later, attention will be posed specifically in works in which the focus is the wind-driving airflow. A first approximation was carried out by Awbi [57]. This author exposed several design considerations for natural convection systems in buildings. He considered the wind for dividing the ventilation modes in three types: single-sided, cross-flow and mixed flow, and proposed a quadratic summation of the volumetric flow rate Q (m^3/s) due to buoyancy (stack) and wind forces:

$$Q = \left(Q_{stack}^{1/n} + Q_{wind}^{1/n} \right)^n \quad (8)$$

being n a factor to be adjusted. In addition, Awbi [57] proposed a relationship for each flow rate with a characteristic pressure difference in each situation (dominant buoyancy or dominant wind).

Summarily, several modes for addressing the problem can be found in the technical literature. For instance, a mathematical procedure has been followed by Ong [58] and Ong and Chow [59], whereas valuable experimental results were obtained by Bouchair [60], Warrington and Ameel [61], Afonso and Oliveira [62], and Onbasioglu and Egrican [63], among others. In some of these works the geometric optimization problem has also been addressed. For example, Bouchair [60] has suggested an aspect ratio of channels about 0.1 for obtaining the maximum ventilating rate, for height $H = 1.95$ m. For the chimney proposed by Bouchair [60], Gan [56] established the following equation for estimating the volumetric flow-rate: $m/\rho = 0.0197 (T_{surface} - T_{air,inlet})^{0.4015}$. It is patent that numerical simulation has been gaining more importance in recent years, as will be seen later.

5. Overview of Relevant Literature

Several valuable articles containing detailed reviews on different aspects of the regarded problem can be found in literature, and a discussion of some of them follows. Stevanović [64] has carried out an exhaustive review of studies on simulation-based optimization of passive solar strategies of design, focusing on the optimization methods and software employed in literature. This author has presented summaries of research on the optimization of building form, of opaque envelope components, of glazing and shading elements, as well as on the passive solar design of whole buildings. Note that although passive solar devices such as solar chimneys or Trombe walls are part of the general research, here the focus is mainly on the design of the building itself. Therefore, the materials used in the building construction, the thickness of the insulating walls, the evaluation of the irradiation received and thus the solar orientation, or the heating or cooling needs of the dwellings, among others, are factors to be considered in this type of study. The problem is multidisciplinary, and in addition the numerical and parametric methods different optimization algorithms have been used, such as those of *genetic* type, or *neural networks*, for instance.

In the review by Zhan et al. [65], the concept of Air Layer Involved Envelopes (ALIEs) is extended to multiple applications in buildings envelopes: multi-layer door/windows,

double-skin façades, solar collectors, Trombe walls, solar chimneys, etc. These authors divided the air layers applications into:

Air layer employed in external walls: single Trombe wall and composite Trombe wall, ventilated (double-skin glazing) façades, wall-based solar chimneys, glazed and unglazed transpired solar walls, ventilated PhotoVoltaic (PV), façades, vertical greenery walls, double layer walls, . . .

Air layer utilized in windows: multiple panel windows, ventilated windows, . . .

Air layer employed in roofs: ventilated roofs, roof solar chimneys, solar air heaters integrated in roofs, . . .

Omrany et al. [66] presented a review on the application of passive wall systems for improving building efficiency. They explored the potential of different passive wall systems for improving thermal performance through the reduction in consumptions in buildings. They pointed out that the Trombe wall is recognized as a system for achieving the above purpose, and therefore careful analysis of design parameters can contribute to improving the thermal performance of systems. As the main objective of the review by Zhan et al. [65] is to show the existing applications and technologies of air layers at walls (of buildings), the searching of better thermal or dynamic behavior of passive solar devices is not deserved a particular attention. Something similar occurs with the survey by Omrany et al. [66].

A review was carried out by Zhai et al. [67] focused on solar chimneys in buildings. Although geometry or shape optimization are not specially treated, some relevant data taken from literature over dimensions and ventilation capacity are exposed throughout the work. Zhai et al. [67] suggested in their conclusions that it is interesting to combine the solar chimney systems with natural cooling systems, such as underground cooling, evaporative cooling, and others. In addition, the performance of solar chimneys for ventilation can also be enhanced with solar cells and solar collectors.

Shi et al. [68] have presented an overview on the influencing performance factors in solar chimneys in buildings. From results reported in literature, these authors pointed out that a solar chimney under solar radiation can achieve better performance with cavity gap of 0.2–0.3 m, aspect ratio of around 10, equal inlet and outlet areas, and in the case of roof solar chimney inclination angle in the range 45–60°, considering latitude. In addition, the corresponding room should have appropriate openings, double or triple glazing, thick insulation at the wall of 5 cm, and solar absorber with high values of absorptivity and emissivity. They organized the work in:

Influences of configuration (height, cavity gap, inlet and outlet areas, . . .)

Influences of installation conditions (inclination angle, room opening, solar collector)

Influences of material usages (type of glazing, materials for solar absorber, thermal insulation . . .)

Influences of environment (solar radiation, external wind . . .)

Recently, Zhang et al. [69] have conducted a review on solar chimney applications in buildings, focusing on the influencing factors of performance and the works developed at RMIT University of Australia. They have suggested several potential trends and challenges in solar chimneys for achieving enhancements.

6. Solar Chimneys: Topics

6.1. Prevailing Buoyancy

Focusing more specifically on solar chimneys, note that depending on the proposed design or the intended function, solar chimney can be classified under different denominations (thermosiphons, Trombe wall, and others), ingredients such as natural ventilation, solar radiation, and *buoyancy-driving* or *wind-driving forces* are presented to a greater or lesser extent (see Figure 4). A considerable body of work dealing with airflows induced only by buoyancy (or *stacks*) effects can be found in the literature. Ding et al. [70], Mathur et al. [71,72], Burek and Habeb [73] and Arce et al. [74] experimentally analyzed the performance of solar chimneys for ventilation purposes. In their experiments in a standard L-shaped (vertical) solar chimney, Mathur et al. [71] found a potential for inducing ven-

tilation in the range 50–150 m³/h volumetric airflow-rate for 300–700 W/m² irradiation on the vertical surface, whereas in [72], for an inclined solar chimney placed at rooftop of room, authors reported that optimum inclination was in the range 40–60°, depending upon latitude. Burek and Habeb [73], from their experimental results, suggested that mass-flow rate m within the channel in solar chimneys and Trombe walls devices could be approximated by $m \sim (\text{heat input})^{0.572}$, and $m \sim b^{0.712}$.

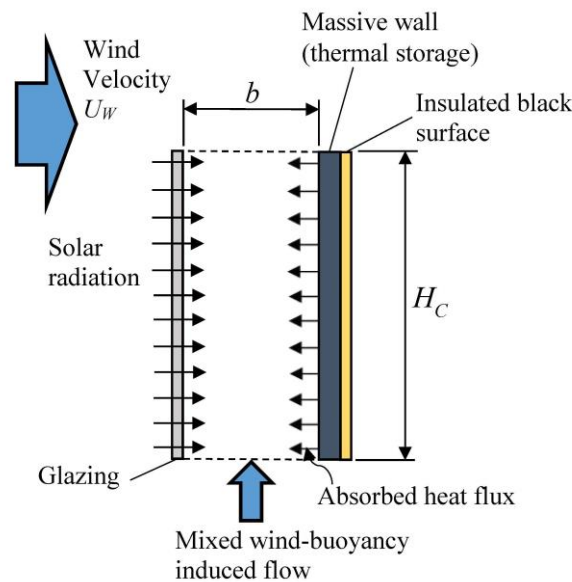


Figure 4. General arrangement of the thermally active walls forming main channels in a solar chimney system.

As noted above, numerical simulation has been widely used in the study of systems of interest. Bacharoudis et al. [75] reported numerical solutions for the airflow established in a wall solar chimney by asymmetrical heating. For simulating the turbulence they used the *standard* k - ϵ model, the *realizable* k - ϵ model, the RNG k - ϵ model, the *Reynolds Stress Model* (RSM), and two different low-Re models. It was concluded that use of low-Re turbulence models assures the prediction of realistic velocity and temperature profiles. Best approximation to the experimental results was reached by using the realizable k - ϵ turbulence model. Harris and Helwing [76] reported numerical results obtained through Phoenics finite-volume code for a simple solar chimney, finding that the optimum slope was equal to 67.5° for obtaining maximum airflow rate.

Bassiouny and Koura [77] carried out an analytical and numerical study of a solar chimney attached to a room. They encountered that the absorber average temperature could be correlated as a function of the solar intensity I (W/m²) as $T_w = 3.51 I^{0.461}$, whereas the average exit velocity could be approximated by $V_{exit} = 0.013 I^{0.4}$.

More recently, Zhang et al. [78] have presented a numerical study of a wall solar chimney for ventilating multi-zone buildings, focusing on multiple connected rooms. They have determined that the optimal design requires a solar chimney with cavity gap of 0.2 m, and an inlet size also equal to 0.2 m. These authors pointed out that the design of inlet position and chimney height can significantly affect the overall performance of the device. Numerical simulation has been addressed through the Fire Dynamics Simulator (FDS) code, based on a LES procedure. This CFD code was also used by Shi and Zang [79] in their investigations; from numerical results, these authors proposed different relationships for the established air-flow rate, of the type $m/\rho = A_{open}/(0.65 + 5.2A_{open})$, being A_{open} the opening area of device.

Jiménez-Xamán et al. [80] have reported numerical results to describe the behavior of a rooftop solar chimney attached to a single room. They have employed a CFD numerical model considering the surface thermal radiation exchange between (internal) room walls, and a pseudo-interaction of exterior boundary conditions with conducting walls.

The resulting local velocities varied in the range 0.16 to 0.22 m/s in summer and winter conditions. Vázquez-Ruiz et al. [81] have numerically analyzed the influence of the solar roof chimney position on the heat transfer in rooms. Numerical results obtained by means of ANSYS Fluent were successfully compared to experimental data. They have encountered relevant differences in the thermal behavior of devices for different locations of the rooftop solar chimney. The work of Lee and Strand [82] can stand as representative of alternative numerical procedure. Based on an analytical approach of the problem, a parametric study has been developed through the EnergyPlus code. They encountered mass-flow rate increases above 70% when the chimney height increases from 3.5 to 9.5 m. However, they have not found relevant differences in mass-flow rate as a function of the air gap width, at least in the range $b = 0.15\text{--}0.75$ m.

Additional aspects of the problem can be found in literature. For instance, the *solar air heaters* are simple devices that capture the solar radiation to heat the air at ambient conditions, and thus using this warm air for conditioning buildings (see works of Singh et al. [83,84]). Obviously, the advances in different solar passive devices such as Trombe walls are applicable to solar chimneys. Zhang et al. [85] reported a numerical study on investigating the heating behavior of an improved Trombe wall, previously investigated experimentally. Through a three-dimensional model implemented in a commercial CFD software, the heating characteristics between the proposed Trombe wall and a traditional one have been compared. In the analysis, effects of irradiation, ambient temperature, absorptivity and emissivity of the wall's materials, and the gap of the air channel, have been addressed. They encountered that the best heating performance takes part with a height of 2.7 m and the gap of air channel ranged from 70 to 80 mm.

Recently, Liu et al. [86] have reported a contrastive analysis of a combined solar chimney that can be utilized for both winter heating and summer ventilation. They have focused on the feasibility and applicability of several operational modes of three different structural solar chimneys. Numerical results have been obtained through CFD techniques, using the realizable $k\text{--}\varepsilon$ model for turbulence. The ANSYS Fluent finite-volume code has been employed by Nguyen et al. [87] for conducting an analysis of different strategies for a room with a heated wall, with typical solar chimney geometry. As a novelty, a double vertical channel is considered; in some cases, the authors encountered very relevant increases in ventilation rates by changing the morphology and the heating conditions of the device.

6.2. Taking into Account Radiative Effects

As indicated throughout the manuscript, depending on the procedure for addressing the problem, boundary conditions at walls have been treated as adiabatic, or imposing fixed values of temperature and/or heat flux, or alternately by modeling of the *real* heat fluxes at walls: irradiation, conduction, convection, radiation between heated walls, etc. If this treatment is adopted, thermal and radiative properties of participating materials (thermal conductivity, emissivity, absorptivity, etc.) should be included in the analysis. However, the resulting study could not be generalist enough, but depending on the *realistic* materials involved in the analysis. Obviously, it is possible to find multiple treatments in technical literature. A compromise solution could consist of simplifying the boundary conditions at walls sufficiently, along with retaining *radiative effects* between walls when they are considered as relevant (i.e., surface thermal radiation).

The radiative heat transfer has not been included in most cases found in literature because it can be considered negligible compared to the convective (or even conductive) effects. However, thermal radiation should not be neglected in some cases, and therefore different studies have been conducted by several authors (in our field, Nouanégué and Bilgen [88], Montiel et al. [89], for instance). Both the radiative and the variable thermophysical properties of fluid have been analyzed in detail by Zamora and Kaiser [90], for cavities with thermal passive configuration. For a morphology corresponding to a solar chimney attached to a room, these authors quantified the relevance of the commented effects, and

determined the range of parameters (for instance, the heating intensity, $\Lambda = \Delta T/T_\infty$) for which discrepancies in the obtained numerical results were important. They used the IMMERSOL model of Spalding that is provided in Phoenics code. Usually, the radiation effects can be restricted in numerical simulations to surface-to-surface radiation as aforementioned), which has offered successful results validated with experimental data (i.e., air assumed as transparent to radiation). Different models have been employed such as the *Rosseland diffusion* approach, the *radiosity-irradiance* or the *composite-radiosity* models, or the *six-flux radiation* formulation, for instance.

6.3. Wind-Driving Effects

In the following, the attention is focused on the impact of the wind on a solar chimney. In real situations both wind forces and buoyancy (or stack) forces induce the airflow, as explained before. In some cases, the ventilation rate originated by the combination of these two effects can be higher than that obtained only by buoyancy forces. However, under given conditions effects may oppose each other and not necessarily enhance the total ventilation rate. It can be concluded that each configuration should be analyzed separately for realistically knowing the relevance of different effects. Contributions by Awbi [57] and Bansal [91] can be considered as pioneering. As aforementioned, Awbi [57] proposed that the mass-flow rate could be obtained through correlations for each separate driving force, for engineering applications. Nouanégué et al. [92] considered that the upper opening of the solar tower was oriented against the cardinal direction of wind to obtain a depression area most of the time. They presented numerical results of mixed convection airflow for simulating the effects of wind, and presented the results of Nusselt number and ventilation rate as a function of Ra/Re^2 , i.e., the Richardson number.

Zamora and Kaiser [93] conducted a numerical study on mixed buoyancy-wind driving airflow induced in a solar chimney, aiming for building ventilation. They detected a gap in the study of ventilation by means of solar chimneys subject to wind. For low enough Rayleigh numbers, buoyancy effects were almost insignificant compared to wind forces, except for low enough values of wind velocity. For high values of the Rayleigh number wind effects became dominant from velocities 1–2 m/s, whereas for 2–3 m/s, wind effects were always prevalent. From numerical results obtained through the Phoenics code they proposed a global correlation for ventilation rate m , involving the velocity speed and the characteristic buoyancy velocity as a function of Rayleigh number.

The influence of wind speed and direction on the performance of a particular solar chimney have been addressed by Neves and da Silva [94], who confirmed the importance of analyzing the combined effects of natural convection and wind-driven ventilation. As pointed out by Zamora and Kaiser [93], aeromotive forces do not always produce a positive effect. Under certain circumstances the depression that usually appears at the outlet of the solar towers tends to decrease, and then the ventilation rate could also decrease. In fact, Neves and da Silva [94] investigated the effects of wind speed and direction on the performance of a solar chimney placed at the roof of an experimental cell, involving a cover at the outlet opening; they encountered a reduction of up to 47% in the volumetric flow-rate through the chimney due to the opposite incidence of wind to the inlet opening, even for relatively low values of wind such as 0.6 m/s. In addition, these authors presented results for wind pressure and discharge coefficients.

The interference of wind on solar chimneys attached to a building have been also analyzed by Shi [95], both theoretically and numerically through the FDS code, who suggested that a higher wind velocity does not induce a better solar chimney performance, which is dependent on the wind incidence angle with respect the outward normal of the wall with the window (keep in mind that this author has reproduced a typical building). Again, Shi [95] confirmed that the interaction of atmospheric wind cannot be neglected in the behavior of solar chimneys when practical applications are addressed.

Predictions for solar chimneys' performance under buoyancy effects exclusively can be strongly modified when wind forces are relevant, as pointed out by Wang et al. [96]. The

non-inclusion of wind effects can produce a clear underestimation of ventilation rates in most cases. Numerical results were obtained through the CFD FDS code, including the radiative heat transfer. Keeping in mind the wind effects for solar chimneys dedicated to ventilation purposes, elements such *windcatchers* deserve to be analyzed. Nouanégué et al. [94] studied the integration of windcatchers with solar chimneys through a numerical investigation. Moosavi et al. [97] analyzed both numerically and experimentally the performance of a windcatcher combined with a solar chimney, in conjunction with a water spray system, for a two-story office building in an arid and warm climate. A comprehensive review on natural ventilation aided by windcatchers has been carried out by Jomehzadeh et al. [98].

Evola and Popov [99] presented a CFD analysis of wind-driven natural ventilation in a building with single-side ventilation and an opening in the windward wall. They employed the RNG $k-\epsilon$ turbulence model, finding a good agreement with numerical LES and experimental results taken from literature. As expected, these authors encountered difficulties with the standard $k-\epsilon$ model in describing the airflow close the surfaces, in which the damping of kinetic energy is relevant. Pakari and Ghani [100] reported an assessment in the airflows in a ventilated greenhouse equipped with wind towers, both numerically and experimentally (wind tunnel facility). They pointed out that for wind velocities above 2 m/s, the volumetric flow-rate was enough for regulating the air temperature within the greenhouse.

6.4. Fundamentals of Wind Numerical Simulation

Special attention deserves the appropriate numerical simulation of the wind in realistic conditions. Assuming a given uniform velocity for the incident wind is often not adequate for simulating the performance of solar chimneys and Trombe walls under given circumstances. An analysis on the impact of several parameters on CFD simulations of cross-ventilation has been conducted by Ramponi and Blocken [101], for a generic isolated building. The focus was posed on the boundary conditions imposed for CFD simulations of the turbulent flow, for achieving accurate enough predictions of the atmospheric airflows involved in ventilation of buildings. Similarly, Park et al. [102] have presented numerical studies to analyze the combined effects of both stack and wind forces on windward single-side ventilation. In view of the relevant influence of the acting wind forces on any passive thermal system, in the last cited works (as well as others found in the literature) it is evident that the encouragement was for the authors to perform a physically adequate numerical simulation of the Atmospheric Boundary Layer (ABL).

The atmospheric wind can be introduced through a logarithmic profile, giving the distribution of horizontal wind speed U_W as a function of vertical coordinate y , as:

$$U_W(y) = \frac{u_\tau}{k_v} \ln\left(\frac{y}{y_0}\right) \quad (9)$$

being u_τ the total friction velocity, k_v the von Kármán turbulent constant (≈ 0.41) and y_0 the effective roughness height of the ground terrain. Grimmond and Oke [103] and Blocken et al. [104], for instance, have provided different values for y_0 , depending on the ground type.

In this way, for simulating the ABL correctly by means of standard two-equations models of turbulence in CFD procedures, the following distributions of turbulent variables should be imposed:

$$k = \frac{u_\tau^2}{(C_\mu C_d)^2}; \quad \epsilon(y) = \frac{u_\tau^3}{k_v y}; \quad \omega(y) = \frac{\epsilon}{(C_\mu C_d) y} \quad (10)$$

which are based on the formulation proposed by Richards and Hoxey [105], with $C_\mu = 0.5478$ and $C_d = 0.1643$, as the usual constants in turbulence models. According to these profiles fixed values of k , ϵ and ω should be applied at the top free of the computational domain.

The idea is to include a sufficiently large computational domain in the numerical analysis, so that the blowing wind over the building is simulated from the limits through the boundary conditions. For large computational domains, this can reveal the problem of the

appropriateness of boundary conditions and the non-homogeneity of properties profiles in a horizontal direction in the ABL. This has been repeatedly analyzed in literature (Blocken et al. [106], or Richards and Norris [107], among others). Really, the problem emerges when the height roughness related to the rough wall-function is based on the sand-grain roughness of Nikuradse; this is the case of ANSYS Fluent code, and the aforementioned authors have provided rules for avoiding the problem. In turn, the ABL is well simulated in Phoenics code, with the only prevention being that physically the value of effective roughness height should not be greater than the distance between the first computational node of mesh and the ground.

Van Hoof et al. [108] have developed a validation of cross-ventilation flow through a generic isolated building for five RANS turbulence models and for a LES model based on the dynamic Smagorinsky subgrid-scale model. In the specification of wind boundary conditions, these authors have considered the rules given above. An indication that the problem may become numerically complex is that the five different steady RANS models provided significantly different results. Depending on the type of problem, RANS results could approximate to LES results (intrinsically transient), but for obtaining sufficient accuracy, use of LES models involves an increase in computational time with a factor of 80–100 in turn. In general, the use of LES has produced a higher agreement with the experimental results.

Lastly, it may be interesting to have practical correlations to evaluate the convection coefficients when the wind is blowing over passive thermal structures, avoiding more detailed calculations, especially for designers. Palyvos [109] has presented a valuable survey. Other similar contributions can be found in literature.

7. Solar Chimneys: Shapes and Designs

7.1. Shapes and Designs. Background

Improving the performance of systems based on solar chimneys has been the subject of intense study in recent years. From a systemic point of view, it seems clear that the combined use of several technologies can lead to the achievement of optimal operating conditions for each case. Zhang et al. [110] pointed out in their critical review that the combination of solar chimneys, Trombe walls, double-skin façades, solar roof collectors, photovoltaic (PV) panels, evaporative or adsorption cooling components, even including phase change materials, and more, constitutes a powerful strategy for achieving the fundamental objectives of energy saving and global warming reduction. Therefore, the number of aspects and articles published on the different facets of the problem is enormous. The wind impact deserves appropriate attention; in fact, new design proposals appear, such as that explained by Shaeri and Mahdavinjad [111]. These authors have placed an aerodynamic form above the wind chimney, taken from the shape of an aircraft wing. The form is used upside down according to the required performance; low air pressure is generated below it when the wind is blowing. Numerical results are obtained by means of COMSOL Multiphysics: a parametric optimization procedure drive to obtain the best location of the aerodynamic form to produce the best wind chimney performance.

Following, three main fields are specifically reviewed: tilt-related, width-related, and inlet/outlet-related studies.

7.2. Tilt-Related Studies

Constructively, optimizing the slope angle of the walls forming a solar chimney has more sense for rooftop-type chimneys (Figure 5). The optimum tilt or slope of solar chimneys for obtaining the maximum airflow was studied by Harris and Helwing [76]. They proposed an optimum slope equal to 67.5° , as aforementioned, for Edinburgh in Scotland at latitude 52° . Sakonidou et al. [112] have conducted an analytical modeling for obtaining the optimum tilt, validating their results with some numerical and experimental results. They reported that the maximum airflow appeared for tilt angles in the range $65\text{--}76^\circ$, whereas for maximum irradiation was $12\text{--}44^\circ$. In the pioneer work of Prasad and

Chandra [113] in India, also analytical, a different trend can be found: $53\text{--}76^\circ$ for maximum airflow, and $0\text{--}55^\circ$ for maximum irradiation. Mathur et al. [72], as commented above, theoretically reported that the optimum slope was in the range $40\text{--}60^\circ$ depending upon latitude; the maximum ventilation rate was encountered of 45° at Jaipur (India) at latitude 27° N. Bassiouny and Korah [114] have found, analytically and numerically, a given range of inclination angles ($45\text{--}75^\circ$) for a latitude of 28.4° , for optimizing the induced mass-flow rate. These authors used the FEM code ANSYS and adopted the Galerkin principle for the weighted residuals function.

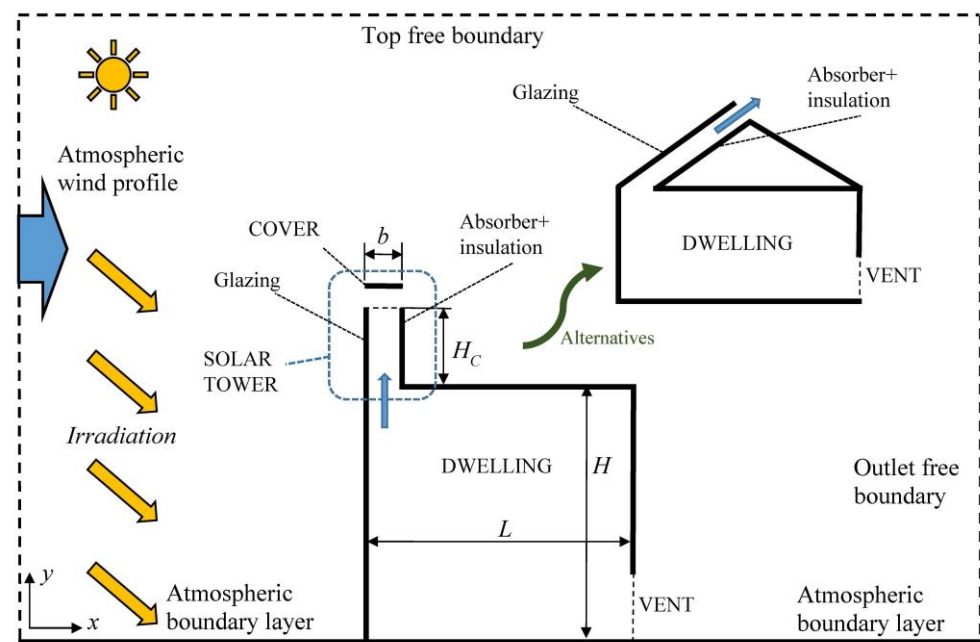


Figure 5. General scheme of a rooftop solar chimney for ventilation purposes. On the right, an alternative configuration for inclined roof is outlined.

The main prevention to be considered when tilting solar chimneys, whether attached to wall rooms or located at the rooftop, will be explained in the following. The inclination of walls with respect to vertical direction, in which buoyancy forces are acting, can lead to the occurrence of *reverse flow*. Consequently, this fact could result in a reduction in the induced total mass-flow rate through the solar chimney, not desirable for ventilation applications. This topic has been treated by Khanal and Lei, both numerically [115] and experimentally [116], for an inclined wall solar chimney with a uniform heat flux at the thermally active wall; experiments showed that reversal flow should be minimized for obtaining better performance conditions. The optimal inclination angle was considerably low (of the order of 5° with respect to vertical direction). Ren et al. [117] have studied the problem numerically, confirming the negative effects of the reversal flow presence on inclined solar chimneys. They have proposed an inclined solar chimney (of rooftop type) including discrete heat sources integrated at the exterior skin of the structures for suppressing the reverse flow. They have encountered that the optimal inclination angle maximizing the ventilation rate strongly depends on the Rayleigh number.

Kong et al. [118] have developed a CFD based approach for identifying the optimum inclination angle of rooftop solar chimneys for different real climate zones in Australia. They revealed that the best performance conditions for ventilation occurred for slopes in the range 45° to 60° , depending on the operation latitude and season. Wind direction and wind speed are not included in the study, although the authors recognize that they should be analyzed in future works.

7.3. Width-Related Studies

Another morphological factor for optimizing the thermohydraulic performance of solar chimneys is the wall-to-wall distance of the space occupied by fluid. The physical reasoning of the existence of a maximum has been already treated, and several works have been discussed, mainly for simplified geometries [29,31], but also including geometries oriented to solar passive systems [45] and even for the solar chimneys themselves [78,82].

Zavala-Guillén et al. [119] have presented an analysis of the conjugate heat transfer on a double air-channel solar chimney, aiming to obtain the configuration maximizing the induced mass-flow rate for ventilation purposes. These authors have focused on a typical dilemma in the field of interest, consisting of considering given boundary conditions such as isothermal walls, or isoflux or adiabatic walls, or alternately considering effects such as heat conduction and radiation, at least in the glazing wall that transfer the irradiation. In fact, the authors have opted for the latter option and have presented numerical results to carry out a parametric study on the influence of the height and width of the space between the walls occupied by the fluid. They observed that the highest value of the ventilation rate does not correspond to the highest temperature difference. The optimal configuration was for a channel with 2 m in height and 0.125 m wide; thermal efficiency was equal to 38.5% and the mass-flow rate equal to 0.1072 kg/s for an irradiation of 700 W/m².

Regarding the solar chimneys under wind effects, Wang et al. [98], for a solar chimney attached to a room, concluded that the typical values of 0.2–0.3 m of cavity gap for achieving optimal ventilation rate are no longer applicable under the atmospheric wind, and the values rises to 0.4–0.5 m. In general, it should be accepted that these results can be hardly extrapolated to other different geometries, and therefore each morphology deserves particular attention. Relevant differences can be found in the system performance located leeward or windward. Zamora [120] has assessed the performance of three different arrangements of a rooftop solar chimney, through a numerical simulation; particular attention has been paid to the appropriate simulation of the ABL. The author detected that wind produces a decrease in the value of the aspect ratio b/H_C (Figure 5) for better thermal performance. For wind-dominant conditions, the thermal optimal b/H_C was slightly above 0.05; however, the maximum values of the induced mass-flow rate appear asymptotically when b/H_C tends to unity, at least for two of the three regarded configurations. Since no local values of the better dynamic-performance maximizing the ventilation rate was encountered, choosing a wall-to-wall spacing b should be subject to the available space as well as to other constructive considerations. An intermediate value of the aspect ratio could be proposed for achieving the maximum ventilation rate varying the morphology and wind conditions.

7.4. Inlet/Outlet-Related Studies

Regarding the influence of size and shape of the inlet/outlet areas, Al-Kayiem et al. [121] have presented a mathematical analysis of the effects of chimney height and collector area on the performance of a rooftop solar chimney. The considered geometry was double sided inclined absorbers, including a circular cross section chimney pipe. They encountered that even with a large collector area up to 600 W/m² the arrangement was not able to perform feasibly for an irradiation less than 400 W/m² (Malaysian weather conditions). For high enough values or solar radiation, high values of the wind caused a reduction in the system performance, due to increases of losses from the top cover. The influence of the inlet configuration on the performance of the same type of rooftop solar chimney has been analyzed by Al-Kayiem et al. [122]. Numerical results have been obtained through ANSYS Fluent code, including the Discrete Ordinate model for simulating radiative effects. However, the impact of wind has not been included. These authors concluded that best performance was obtained for inlet configuration with vertical cross section.

The author of [123] has considered a C-shaped solar chimney attached to a room, including extended connecting ducts in a horizontal direction. Only buoyancy forces are considered. This author has developed a general model to predict the induced airflows

rates, known as *plume model* (He et al. [124]), validated with experimental results. This analytical model assumes that each thermal boundary layer can be modeled as a one-dimensional plume of constant thickness attached to the walls forming the channel. The channel is therefore divided into the plume flow region and the area outside the plume. The outside region does not contribute to the buoyancy force. In addition, in [125] the flow into the ducts outside the chimney channel is considered as forced flow (thus the model cannot simulate reversal flow). Results have shown that the presence of connecting ducts affects the flow, but no search procedure for the best operating condition is established.

Nguyen and Wells [125] and Nguyen and Nguyen [126] have numerically studied the effects of several configurational factors at the inlet/outlet areas of a vertical solar chimney. They found a strong influence of given configuration changes on the performance of devices.

Fang et al. [127] presented an investigation of a wall-mounted solar chimney system in a single-story building, only under buoyancy driving forces. The effect of the ratio air outlet/air inlet cross-sectional area (S) on the operational effectiveness has been analyzed. ANSYS Fluent code has been employed for conducting the numerical results. They encountered that the maximum local heat flow density reached 188 W/m^2 at $S = 80\%$ and analyzed the relationship between S and the appearance of vortices and secondary flows as well as the influence on the thermal efficiency of the system. Therefore, these authors have concluded that the design of wall-mounted solar chimneys has a non-negligible impact; the proper selection of the S -value range is relevant for the ventilation requirements of engineering design.

Gao et al. [128] have encountered a clear enhancement of a roof solar chimney through the inclusion of a wind-induced channel, which is located at the building's outer wall. In this way, the fluid enters the solar chimney a certain velocity at the upper part and induces the air within to flow upward and pass through the roof. Wind driving forces are retained in the analysis, and numerical results have been presented by using a finite-volume CFD procedure. The new structure improves the ventilation rate due to the wind-induced channel. Authors illustratively explained that when the inclination angle increases from 30° to 90° , the mass-flow rate increases 212% for wind velocity U_W equal to 1 m/s , 166% for $U_W = 2 \text{ m/s}$, and 127% for $U_W = 3 \text{ m/s}$, for an irradiation of 600 W/m^2 .

8. Solar Chimneys: Plates, Fins, and Flow Disturbers

It is expected that the introduction of certain obstacles such as fins, intermediate plates, or turbulence (or vortex) generators (Figure 6), among others, will produce a significant change in the thermohydraulic characteristics of the convective flow. The idea is to analyze the necessary changes in the morphology of the fluid flow zones, seeking the best operating conditions for passive solar systems.

Changes in the heating conditions can be introduced directly, avoiding obstacles. The effect of discrete heat sources on the natural convection airflow inside an isolated solar chimney has been discussed experimentally and numerically by Ren et al. [117,129]. They encountered that a given distribution of heat sources integrated into the walls enhances the ventilation rate for high enough values of Ra_H . The improvement appears because of discrete sources tending to suppress the reverse flow occurring at the exit of a conventional chimney. For a different geometry with an open-ended channel similar to that formed by the double skin façades with PV panels, Tkachenko et al. [130] have carried out experimental and numerical investigations on the effects of the non-uniformity of the heat flux distribution at walls and have found increases in the induced mass-flow rate for a given arrangement. Numerical results were obtained by using an in-house finite volume solver, validated through comparisons with experimental results. These authors encountered that the introduction of fluctuations at the inlet of the computational domain reveals as necessary for matching the experimental data reasonably. Intermittently fluctuating separations at the entrance drive to the growth of given flow structures produce a clear mixing into the channel.

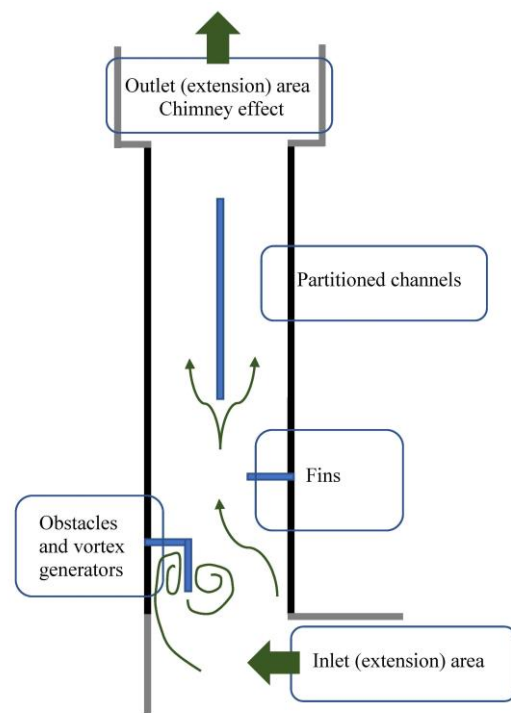


Figure 6. Solar chimney: plates, fins and flow disturbers used in the literature for enhancement behavior proposals.

8.1. Intermediate Plates

Zavala-Guillén et al. [131,132] have considered a channel solar chimney including an intermediate absorber plate. The partitioned arrangement of the channel produced an induced mass-flow rate of up to 50% higher than that obtained in a conventional configuration. Authors have advised that boundary conditions applied to walls forming the partitioned channels, as well as the consideration of radiative and realistic effects, are keys factors for verifying the improvements reached when intermediate plates are included in the analysis.

He and Lv [133] have addressed the idea of improving the efficiency of solar chimneys through the inclusion of transparent glazing insertions into the channel. They have presented experimental and numerical results. Phoenics code has been used, along with the IMMERSOL model for radiative heat transfer, which is unique to Phoenics. Numerically, one insertion of a transparent panel with various solar absorption coefficients can produce a 5 to 9% increase in the mass-flow rate. Experimentally, two insertions increase the mass-flow rate by 30%. As expected, these authors pointed out that the number of insertions should not be excessively high, because of the rising of friction losses that can produce a worsening performance.

Lei et al. [134] have considered introducing a perforated absorber plate into a roof solar chimney to improve the ventilation performance. This plate, which divided the roof solar chimney into two channels, increased the ventilation due to heating the air in the gap, and the consequently increasing the temperature gradient with respect to the ambient. The numerical results have been obtained through CFD modeling with the RNG $k-\epsilon$ turbulence model. Lei et al. [134] verified the results by using the experimental results of a traditional solar chimney studied by Chen et al. [135]. Several slopes (30° , 45° and 60°), as well as widths (0.3, 0.4 and 0.5 m) were considered. An increase up to 35% in the induced mass-flow rate has been obtained with the proposed arrangement, compared to the traditional solar roof chimney. A more relevant effect was obtained for large depth width of the chimney.

Note that the heating conditions assumed for the intermediate plates is a key point for obtaining an eventual enhancement of the ventilation capacity of the solar chimney.

8.2. Fins

Fins are frequently used in forced convection applications, but to a lesser extent in natural convection flows. However, the inclusion of this type of structure attached to the walls forming the channel (Figure 6) can produce in some cases an enhancement mainly of the thermal behavior, and more rarely of the ventilation rate. Wu et al. [136] have carried out a numerical analysis on the impact of fins on a solar Trombe wall. Therefore, attention was posed on the heating capacity of the passive solar system, and not on the ventilation rate. The chosen configuration has been a C-shaped channel. These authors have encountered an increase of 23.7% in the maximum thermal efficiency of the finned Trombe wall compared to the unobstructed one. The enhancement can be obtained with several distributions of fins. Numerical results have been obtained by using ANSYS ICEM code with the RNG $k-\varepsilon$ turbulence model, including radiative effects through the S2S model. These authors have clearly exposed the two opposite effects which can appear. On the one hand, the thermal efficiency increases because of the temperature rising at the outlet section (33.7%), but on the other, the minimum ventilation rate was reduced by 29.9%.

Hoseini et al. [137,138] have tested several shapes of fins mounted on systems related to solar heaters and chimneys. Numerical results have been obtained through CFD simulations employing the Realizable $k-\varepsilon$ turbulence model, and considering the radiative effects by using the S2S model. In the boundary conditions, they have included the convective heat transfer through the corresponding *heat transfer coefficient* h_w ($\text{W}/\text{m}^2\text{K}$):

$$h_w = 5.7 + 3.8 U_W \quad (11)$$

as a function of wind velocity and used extensively in the literature. The considered fin shapes were rectangular, elliptical, and triangular. The better thermal performance was obtained with the inclusion of rectangular fins. Due to having a larger heat transfer surface, the thermal efficiency obtained is clearly higher when the fins are included compared to non-finned channels. In addition, an increase between 7 and 14% in the induced mass-flow rate has been obtained. These authors pointed out that discontinuities such as fins can improve the overall performance of solar chimneys.

8.3. Obstacles and Vortex Generators

A sizeable number of works dealing with the inclusion of obstacles in *solar air heaters* can be found in literature, but studies are scarce when the focus is posed specifically on solar chimneys dedicated to ventilation purposes.

For solar air heaters, Promvong et al. [139] and Ji et al. [140], for instance, have addressed numerical studies for ducts punched delta-winglet vortex generators (the first), and for the device roughened by multiple V-shaped ribs (the second). The main objective was the thermohydraulic efficiency enhancement, and this was achieved in both cases. In these works, and others found in literature, the analysis of the flow structures and the influence of the generated vortices on the behavior of systems revealed the importance of achieving the complete knowledge of the problem. However, the numerical simulations haven't been conducted by imposing forced convection conditions through a given air velocity at the inlet of the narrow channels. In a similar line, Arunkumar et al. [141] have checked the influence of the inclusion of helicoidal spring-shaped fins also into solar air heaters. Unfortunately, results obtained for this type of geometry can hardly be extrapolated to systems based on natural convection in solar chimneys attached to buildings or placed on the roofs.

For both forced and natural convection, the effects of thermal diffusion in developed boundary layers produce a certain stabilization of the heat transfer process, and thus can be considered as an obstacle for improving the efficiency of the system. A strategically placed obstacle can cause a disturbance in the boundary layers attached to the thermally active walls, increase the level of turbulence, or even produce vortex shedding which can ultimately increase the heat transfer between the fluid and the walls. The generation of

alternating vortices can be achieved by the implementation of vibratory or flexible elements, for instance, so it is necessary to develop an appropriate modeling of the fluid-structure interaction for the numerical simulation of airflow (Shi et al. [142], among others). However, it is commonly accepted in the concerned literature that the use of vortex generators produces higher pressure loss, and therefore a greater pumping power is mandatory to obtain the same mass-flow rate in forced convection problems. For natural convection problems it is physically understood that the induced mass-flow rate will decrease, mainly due to the reduction in the section available for the fluid flow. In other words, it can be expected that in most cases the increase in buoyancy forces because of the disturbance caused in the boundary layers and the mixing effects could not compensate for the obstructive impact of immersed bodies. Therefore, the ventilation capacity of solar chimneys installed in dwellings and buildings can even decrease drastically, which could produce higher heat transfer coefficients.

A relatively low number of studies on this subject have been found in the literature, when specifically discriminating on solar thermal chimneys. Nguyen et al. [143] have numerically examined the effect of a rectangular obstacle placed at the heated surface of an intermediate plate in a solar chimney. They have found that the thermal efficiency increase was up to 13%. These authors have employed the ANSYS Fluent code with the RNG $k-\varepsilon$ turbulence model. Works reported by Gandjalikhan et al. [144] and Sheikhnejad and Nassab [145] are noteworthy. These authors have achieved a clear thermal enhancement of a solar air heater (with natural convection airflow) and of a solar chimney, respectively. They have embedded an elastic porous winglet, also known as *porous vortex generator*. The problem approach is passive, but they considered that the problem must be addressed in transient two-manner coupled Fluid-Structure Interaction (FSI) condition. The CFD code used is COMSOL Multiphysics (based on finite element method). Finally, Sheikhnejad and Nassab [145] have recognized that using turbulence generators is recommended for the thermal behavior mode of the solar chimney, but not for its use for ventilation mode since the induced mass-flow rate has been lower.

9. Short Note on the Influence of Climatic Conditions

Throughout the manuscript it has been shown that climatic conditions and latitude are decisive factors in the operation of solar chimneys and therefore the efficiency. Illustratively, the optimum inclination angle for maximizing the ventilation rate depends on location latitude, and it is well known that solar chimneys are generally considered as unsuitable for regions with low irradiation or very hot/arid climates (Monghasemi and Vadiee [146]).

Maghrabie et al. [147] have pointed out that passive cooling strategies can produce a great challenge, mainly in regions where high temperatures are predominant along the year. The most relevant applications for natural convection solar chimneys take place in residential (and non-residential) buildings, particularly appropriate for hot (moderate) and humid climates. Miyazaki et al. [148] considered a solar chimney integrated into a south façade of a building, under Japanese climate (Tokyo); they showed that the requirement in fan shaft power was reduced by about 50% due to natural ventilation. Chungloo and Limmeechokchai [149] experimentally analyzed the thermal performance of a solar chimney under hot and humid climate conditions (Thailand).

Abdallah et al. [150] have presented a parametric investigation of a solar chimney under Egyptian climate conditions. Authors have claimed that houses in Egypt are design without taking the climate into account enough. Priority of the design presented is to apply during the hot days in summer. Suprasert et al. [151] have conducted numerical simulations through ANSYS Fluent code for investigating the influence of vapor mass fraction in the air-vapor mixture on the air gap of a solar chimney. They encountered that the yield of ventilated airflow was 15.4–26.2% less than that obtained with dry air. Yussof et al. [152] pointed out that stack ventilation is inefficient in the hot and humid climate due to the low temperature gap between the inside and the outside of building. These authors

have proposed a combination of roof collector and vertical solar chimney for enhancing the stack ventilation.

10. Summary

Since the first works reported on the application of the principles of natural convection in solar passive systems for contributing to the air conditioning in buildings, it has created a great interest in the development of new techniques and applications to achieve energy savings in buildings, in just a few decades. The contribution to reducing global warming and greenhouse gases generation constitutes a clear reason for the development of new air conditioning systems for the bioclimatic architecture. Currently, innovative strategies are being developed to achieve the proposed objectives, combining different technologies and operating principles (Monghasemi and Vadiee [148], Zhu et al. [153], Zhang et al. [110], among others).

Regardless of these trends, basic passive air conditioning and ventilation systems such as solar chimneys (and Trombe walls) must continue to be investigated to achieve a general improvement in their thermohydraulic efficiency. It is necessary to conduct more experiments and simulations to solve the basic problems, and to develop their commercial applications. Particularly for solar chimneys, design factors that produce clear thermal improvement are not capable of achieving an improvement in the ventilation capacity, so further research is needed in this regard. In the present work we have focused on the critical review of the improvement proposals that have been reported in the concerned literature, considering different impacts such as wall-to-wall distances or the airflow disturbances caused by obstacles or vortex generators.

Considering that the combination of different passive (and eventually active) air conditioning techniques could increase the economic cost of these systems, which in turn pursue energy savings, it is interesting to try developing basic and relatively simple designs that can achieve the best performance conditions for both the thermal and ventilation requirements.

Funding: This research received no external funding.

Data Availability Statement: Not applicable.

Conflicts of Interest: The author declares no conflict of interest.

References

1. Bejan, A. *Convection Heat Transfer*; Wiley: New York, NY, USA, 1984.
2. Incropera, F.P.; De Witt, D.P. *Introduction to Heat Transfer*; Wiley: New York, NY, USA, 1990.
3. Bejan, A. *Heat Transfer*; Wiley: New York, NY, USA, 1993.
4. Turner, J.S. *Buoyancy Effects in Fluids*; Cambridge University Press: Cambridge, UK, 1973.
5. Yuan, X.; Moser, A.; Suter, P. Wall functions for numerical simulation of turbulent natural convection along vertical plates. *Int. J. Heat Mass Transf.* **1993**, *36*, 4477–4485. [[CrossRef](#)]
6. Versteegh, T.A.; Nieuwstadt, F.T. A direct numerical simulation of natural convection between two infinite vertical differentially heated walls scaling laws and wall functions. *Int. J. Heat Mass Transf.* **1999**, *42*, 3673–3693. [[CrossRef](#)]
7. Henkes, R.A.W.M.; Hoogendorn, C.J. Comparison exercise for computations of turbulent natural convection in enclosures. *Numer. Heat Transf.* **1995**, *28*, 59–78. [[CrossRef](#)]
8. Fedorov, A.G.; Viskanta, R. Turbulent natural convection heat transfer in an asymmetrically heated, vertical parallel-plate channel. *Int. J. Heat Mass Transf.* **1997**, *40*, 3849–3860. [[CrossRef](#)]
9. Wilcox, D.C. *Turbulence Modeling for CFD*, 3rd ed.; DCW Industries: La Cañada, CA, USA, 2006.
10. Peng, S.; Davison, L. Computation of turbulent buoyant flows in enclosures with low-Reynolds number $k-\omega$ models. *Int. J. Heat Fluid Flow* **1999**, *20*, 172–184. [[CrossRef](#)]
11. Xu, W.; Chen, Q.; Nieuwstadt, F.T.M. A new turbulence model for near wall natural convection. *Int. J. Heat Mass Transf.* **1998**, *41*, 3161–3176. [[CrossRef](#)]
12. Ciofalo, M. Large-eddy simulations of turbulent flow with heat transfer in simple and complex geometries using Harwell-FLOW3D. *Appl. Math. Model.* **1996**, *20*, 262–271. [[CrossRef](#)]
13. Salinas-Vázquez, M.; Vicente, W.; Martínez, E.; Barrios, E. Large eddy simulation of a confined square cavity with natural convection based on compressible flow equations. *Int. J. Heat Fluid Flow* **2011**, *32*, 876–878. [[CrossRef](#)]
14. Zhou, Y.; Zhang, R.; Staroselsky, I.; Chen, H. Numerical simulation of laminar and turbulent buoyancy-driven flows using a lattice-Boltzmann based-algorithm. *Int. J. Heat Mass Transf.* **2004**, *47*, 4869–4879. [[CrossRef](#)]

15. Nokhosteen, A.; Sobhansarbandi, S. Utilizing lattice Boltzmann method for heat transfer analysis in solar thermal systems. *Sustain. Energy Technol. Assess.* **2021**, *46*, 101264. [[CrossRef](#)]
16. Gray, D.D.; Giorgini, A. The validity of the Boussinesq approximation for liquids and gases. *Int. J. Heat Mass Transf.* **1976**, *19*, 545–551. [[CrossRef](#)]
17. Zhong, Z.Y.; Yang, K.T.; Lloyd, J.R. Variable property effects in laminar natural convection in a square enclosure. *ASME J. Heat Transf.* **1985**, *107*, 133–138. [[CrossRef](#)]
18. Emery, A.F.; Lee, J.W. The effects of property variations on natural convection in a square enclosure. *ASME J. Heat Transf.* **1999**, *121*, 57–62. [[CrossRef](#)]
19. Chenoweth, D.R.; Paolucci, S. Natural convection in an enclosed vertical air layer with large horizontal temperature differences. *J. Fluid Mech.* **1986**, *169*, 173–210. [[CrossRef](#)]
20. Guo, Z.Y.; Wu, X.B. Thermal drag and critical heat flux for natural convection of air in vertical parallel plates. *ASME J. Heat Transf.* **1993**, *115*, 124–129. [[CrossRef](#)]
21. Guo, Z.Y.; Song, Y.Z.; Li, Z.X. Laser speckle photography in heat transfer studies. *Exp. Thermal Fluid Sci.* **1995**, *10*, 1–16. [[CrossRef](#)]
22. Elenbaas, W. Heat dissipation of parallel plates by free convection. *Physica* **1942**, *9*, 1–8. [[CrossRef](#)]
23. Aihara, T. Effects of inlet boundary conditions on numerical solutions of free convection between vertical parallel plates. *Rep. Inst. High Speed Mech.* **1973**, *28*, 258.
24. Kettleborough, C.F. Transient laminar free convection heated vertical plates including entrance effects. *Int. J. Heat Mass Transf.* **1972**, *15*, 883–896. [[CrossRef](#)]
25. Nakamura, H.; Yutaka, A.; Naitou, T. Heat transfer by free convection between two parallel flat plates. *Numer. Heat Transf.* **1982**, *5*, 95–106. [[CrossRef](#)]
26. Desrayaud, G.; Chénier, E.; Joulin, A.; Bastide, A.; Brangeon, B.; Caltagirone, J.P.; Cherif, Y.; Eymard, R.; Garnier, C.; Giroux-Julien, S.; et al. Benchmark solutions for natural convection flows in vertical channels submitted to different open boundary conditions. *Int. J. Therm. Sci.* **2013**, *72*, 18–33. [[CrossRef](#)]
27. Wong, S.C.; Chu, S.H. Revisit on natural convection from vertical isothermal plate arrays-effects of extra plume buoyancy. *Int. J. Therm. Sci.* **2017**, *120*, 263–272. [[CrossRef](#)]
28. Bodoia, J.R.; Osterle, J.F. The development of free convection between heated vertical plates. *ASME J. Heat Transf.* **1962**, *84*, 40–44. [[CrossRef](#)]
29. Bar-Cohen, A.; Rohsenow, W.M. Thermally optimum spacing of vertical, natural convection cooled, parallel plates. *ASME J. Heat Transf.* **1984**, *106*, 116–123. [[CrossRef](#)]
30. Anand, N.K.; Kim, S.H.; Fletcher, L.S. The effect of plate spacing on free convection between heated parallel plates. *ASME J. Heat Transf.* **1992**, *114*, 515–518. [[CrossRef](#)]
31. Zamora, B.; Hernández, J. Influence of upstream conduction on the thermally optimum spacing of isothermal, natural convection-cooled vertical plate arrays. *Int. Commun. Heat Mass Transf.* **2001**, *28*, 201–210. [[CrossRef](#)]
32. Zamora, B. Thermally optimum spacing between inner plates in natural convection flows in cavities by numerical investigation. *Processes* **2020**, *8*, 554. [[CrossRef](#)]
33. Haaland, S.E.; Sparrow, E.M. Solutions for the channel plume and the parallel-walled chimney. *Num. Heat Transf.* **1983**, *6*, 155–172. [[CrossRef](#)]
34. Straatman, A.G.; Tarasuk, J.D.; Floryan, J.M. Heat transfer enhancement from a vertical, isothermal channel generated by the chimney effect. *ASME J. Heat Transf.* **1993**, *115*, 395–402. [[CrossRef](#)]
35. Morrone, B.; Campo, A.; Manca, O. Optimum plate separation in vertical parallel-plate channels for natural convective flows: Incorporation of large spaces at the channel extremes. *Int. J. Heat Mass Transf.* **1997**, *40*, 993–1000. [[CrossRef](#)]
36. Ledezma, G.A.; Bejan, A. Optimal geometric arrangement of staggered vertical plates in natural convection. *ASME J. Heat Transf.* **1997**, *119*, 700–708. [[CrossRef](#)]
37. Viswamula, P.; Ruhul Amin, M. Effects of multiple obstructions on natural convection heat transfer in vertical channels. *Int. J. Heat Mass Transf.* **1995**, *38*, 2039–2046. [[CrossRef](#)]
38. Zhang, X.; Liu, D. Optimum geometric arrangement of vertical rectangular fin arrays. *Energy Convers Manag.* **2010**, *51*, 2449–2456. [[CrossRef](#)]
39. Ben Maad, R.; Belghith, A. The use of grid-generated turbulence to improve heat transfer in passive solar systems. *Renew. Energy* **1992**, *2*, 333–336. [[CrossRef](#)]
40. Bejan, A. *Shape and Structure, from Engineering to Nature*; Cambridge University Press: Cambridge, UK, 2000.
41. Bejan, A.; Lorente, S. The constructal law and the thermodynamics of flow system with configuration. *Int. J. Heat Mass Transf.* **2004**, *47*, 3203–3214. [[CrossRef](#)]
42. Da Silva, A.L.; Lorenzini, G.; Bejan, A. Distribution of heat sources in vertical channels with natural convection. *Int. J. Heat Mass Transf.* **2005**, *48*, 1462–1469. [[CrossRef](#)]
43. Da Silva, A.K.; Gosselin, L. Optimal geometry of L and C-shaped channels for maximum heat transfer rate in natural convection. *Int. J. Heat Mass Transf.* **2005**, *48*, 609–620. [[CrossRef](#)]
44. Zamora, B.; Kaiser, A.S. Optimum wall-to-wall spacing in solar chimney shaped channels in natural convection by numerical investigation. *Appl. Therm. Eng.* **2009**, *29*, 762–769. [[CrossRef](#)]

45. Zamora, B.; Kaiser, A.S. Thermal and dynamic optimization of the convective flow in Trombe Wall shaped channels by numerical investigation. *Heat Mass Transf.* **2009**, *45*, 1393–1407. [[CrossRef](#)]
46. Aounallah, M.; Belkadi, M.; Adjlout, L.; Imine, O. Numerical shape optimization of a confined cavity in natural convection regime. *Comput. Fluids* **2013**, *75*, 11–21. [[CrossRef](#)]
47. Biserni, C.; Rocha, L.A.O.; Stanesco, G.; Lorenzini, E. Constructal H-shaped cavities according to Bejan's theory. *Int. J. Heat Mass Transf.* **2007**, *50*, 2132–2138. [[CrossRef](#)]
48. Lorenzini, G.; Biserni, C.; García, F.L.; Rocha, L.A.O. Geometric optimization of a convective T-shaped cavity on the basis of constructal theory. *Int. J. Heat Mass Transf.* **2012**, *55*, 6951–6958. [[CrossRef](#)]
49. Lorenzini, G.; Rocha, L.A.O. Geometric optimization of T-Y-shaped cavity according to Constructal design. *Int. J. Heat Mass Transf.* **2009**, *52*, 4683–4688. [[CrossRef](#)]
50. Linden, P.F. The fluid mechanics of natural ventilation. *Ann. Rev. Fluid Mech.* **1999**, *31*, 201–238. [[CrossRef](#)]
51. Borgers, T.R.; Akbari, H. Free convective turbulent flow within the Trombe wall channel. *Sol. Energy* **1984**, *33*, 253–264. [[CrossRef](#)]
52. Smolec, W.; Thomas, A. Problems encountered in heat transfer studies of a Trombe wall. *Energy Convers Manag.* **1994**, *35*, 483–491. [[CrossRef](#)]
53. Smolec, W.; Thomas, A. Theoretical and experimental investigations of heat transfer in a Trombe wall. *Energy Convers Manag.* **1994**, *34*, 385–400. [[CrossRef](#)]
54. Jubran, B.A.; Hamdan, M.A.; Manfalouti, W. Modelling free convection in a Trombe wall. *Renew. Energy* **1991**, *1*, 351–360. [[CrossRef](#)]
55. Gan, G.; Riffat, S.B. A numerical study of solar chimney for natural ventilation of buildings with heat recovery. *Appl. Therm. Eng.* **1998**, *18*, 117–187. [[CrossRef](#)]
56. Gan, G. A parametric study of Trombe walls for passive cooling of buildings. *Energy Build.* **1998**, *27*, 37–43. [[CrossRef](#)]
57. Awbi, H.B. Design considerations for naturally ventilated buildings. *Renew. Energy* **1994**, *5*, 1081–1090. [[CrossRef](#)]
58. Ong, K.S. A mathematical model of a solar chimney. *Renew. Energy* **2003**, *28*, 1047–1060. [[CrossRef](#)]
59. Ong, K.S.; Chow, C.C. Performance of a solar chimney. *Solar Energy* **2003**, *17*, 1–17. [[CrossRef](#)]
60. Bouchair, A. Solar chimney for promoting cooling ventilation in southern Algeria. *Build. Serv. Eng. Res. Technol.* **1994**, *15*, 81–93. [[CrossRef](#)]
61. Warrington, R.O.; Ameel, T.A. Experimental studies of natural convection in partitioned enclosures with a Trombe wall geometry. *ASME J. Solar Energy Eng.* **1995**, *117*, 16–21. [[CrossRef](#)]
62. Afonso, A.; Oliveira, A. Solar chimneys: Simulation and experiment. *Energy Build.* **2000**, *32*, 71–79. [[CrossRef](#)]
63. Onbasioglu, H.; Egrican, A.N. Experimental approach to the thermal response of passive systems. *Energy Convers. Manag.* **2002**, *43*, 2053–2065. [[CrossRef](#)]
64. Stevanović, S. Optimization of passive solar design strategies: A review. *Renew. Sustain. Energy Rev.* **2013**, *25*, 177–196. [[CrossRef](#)]
65. Zhang, T.; Tan, Y.; Yang, H.; Zhang, X. The application of air layers in building envelopes: A review. *Appl. Energy* **2016**, *165*, 707–734. [[CrossRef](#)]
66. Omrany, H.; Ghaffarianhoseini, A.; Ghaffarianhoseini, A.; Raahemifar, K.; Tookey, J. Application of passive solar systems for improving the energy efficiency in buildings: A comprehensive review. *Renew. Sustain. Energy Rev.* **2016**, *62*, 1252–1269. [[CrossRef](#)]
67. Zhai, X.Q.; Song, Z.P.; Wang, R.Z. A review for the applications of solar chimneys in buildings. *Renew. Sustain. Energy Rev.* **2011**, *15*, 3757–3767. [[CrossRef](#)]
68. Shi, L.; Zhang, G.; Yang, W.; Huang, D.; Cheng, X.; Setunge, S. Determining the influencing factors on the performance of solar chimney in building. *Renew. Sustain. Energy Rev.* **2018**, *88*, 223–238. [[CrossRef](#)]
69. Zhang, H.; Tao, Y.; Shi, L. Solar chimney applications in buildings. *Encyclopedia* **2021**, *1*, 409–422. [[CrossRef](#)]
70. Ding, W.; Hasemi, Y.; Yamada, T. Natural ventilation performance of a double-skin façade with a solar chimney. *Energy Build.* **2005**, *37*, 411–418. [[CrossRef](#)]
71. Mathur, J.; Bansal, N.K.; Mathur, S.; Jain, M.; Anupma. Experimental investigation on solar chimney for room ventilation. *Sol. Energy* **2006**, *80*, 927–935. [[CrossRef](#)]
72. Mathur, J.; Mathur, S.; Anupma. Summer-performance of inclined roof solar chimney for natural convection. *Energy Build.* **2006**, *38*, 1156–1163. [[CrossRef](#)]
73. Burek, S.A.M.; Habeb, A. Air flow and thermal efficiency characteristics in solar chimney and Trombe walls. *Energy Build.* **2007**, *39*, 128–135. [[CrossRef](#)]
74. Arce, J.; Jiménez, M.J.; Guzmán, J.D.; Heras, M.R.; Álvarez, G.; Xamán, J. Experimental study for natural ventilation on a solar chimney. *Renew. Energy* **2009**, *34*, 2928–2934. [[CrossRef](#)]
75. Bacharoudis, E.; Vrachopoulos, M.G.; Koukou, M.K.; Margaritis, D.; Filios, A.E.; Mavrommatis, S.A. Study of the natural convection phenomena inside a solar chimney with one wall adiabatic and one wall under heat flux. *Appl. Therm. Eng.* **2007**, *27*, 2266–2275. [[CrossRef](#)]
76. Harris, D.J.; Helwing, N. Solar chimney and building ventilation. *Appl. Energy* **2007**, *84*, 135–146. [[CrossRef](#)]
77. Bassiouny, R.; Koura, N.S.A. An analytical and numerical study of solar chimney use for room natural ventilation. *Energy Build.* **2008**, *40*, 865–873. [[CrossRef](#)]
78. Zhang, H.; Tao, Y.; Nguyen, K.; Han, F.; Li, J.; Shi, L. A wall solar chimney to ventilate multi-zone buildings. *Sustain. Energy Technol. Assess.* **2021**, *47*, 101381. [[CrossRef](#)]

79. Shi, L.; Zhang, G. An empirical model to predict the performance of typical solar chimneys considering both room and cavity configurations. *Build. Environ.* **2016**, *103*, 250–261. [[CrossRef](#)]
80. Jiménez-Xamán, C.; Xamán, J.; Gijón-Rivera, M.; Zavala-Guillén, I.; Noh-Pat, F.; Simá, E. Assessing the thermal performance of a rooftop solar chimney attached to a single room. *J. Build. Eng.* **2020**, *31*, 101380. [[CrossRef](#)]
81. Vázquez-Ruiz, A.; Navarro, J.M.A.; Hinojosa, J.F.; Xamán, J.P. Effect of the solar chimney position on heat transfer in a room. *Int. J. Mech. Sci.* **2021**, *209*, 106700. [[CrossRef](#)]
82. Lee, K.H.; Strand, R.K. Enhancement of natural ventilation in buildings using a thermal chimney. *Energy Build.* **2009**, *41*, 615–621. [[CrossRef](#)]
83. Singh, A.P.; Akshayveer; Kumar, A.; Singh, O.P. Designs for high flow natural convection solar air heaters. *Sol. Energy* **2019**, *193*, 724–737. [[CrossRef](#)]
84. Singh, A.P.; Akshayveer; Kumar, A.; Singh, O.P. Natural convection solar air heater: Bell-mounted integrated converging channel for high flow applications. *Build. Environ.* **2021**, *187*, 107367. [[CrossRef](#)]
85. Zhang, L.; Dong, J.; Sun, S.; Chen, Z. Numerical simulation and sensitivity analysis on an improved Trombe wall. *Sustain. Energy Technol. Assess.* **2021**, *43*, 100941. [[CrossRef](#)]
86. Liu, H.; Li, P.; Yu, B.; Zhang, M.; Tan, Q.; Wang, Y.; Zhang, Y. Contrastive analysis on the ventilation performance of a combined solar chimney. *Appl. Sci.* **2022**, *12*, 156. [[CrossRef](#)]
87. Nguyen, A.Q.; Nguyen, V.T.; Tran, L.T.; Wells, J.C. CFD analysis of different ventilation strategies for a room with a heated wall. *Buildings* **2022**, *12*, 1300. [[CrossRef](#)]
88. Nouanégué, H.F.; Bilgen, E. Heat transfer by convection, conduction and radiation in solar chimney systems for ventilation of dwellings. *Int. J. Heat Fluid Flow* **2009**, *30*, 150–157. [[CrossRef](#)]
89. Montiel, M.; Hinojosa, J.; Estrada, C.A. Numerical study of heat transfer by natural convection and surface thermal radiation in an open cavity receiver. *Sol. Energy* **2012**, *86*, 1118–1128. [[CrossRef](#)]
90. Zamora, B.; Kaiser, A.S. Radiative and variable thermophysical properties effects on turbulent convective flows in cavities with thermal passive configuration. *Int. J. Heat Mass Transf.* **2017**, *109*, 981–996. [[CrossRef](#)]
91. Bansal, N.K.; Mathur, R.; Bhandari, M.S. A study of solar chimney assisted wind tower system for natural ventilation in buildings. *Build. Environ.* **1994**, *29*, 495–500. [[CrossRef](#)]
92. Nouanégué, H.F.; Alandji, L.R.; Bilgen, E. Numerical study of solar-wind tower systems for ventilation of dwellings. *Renew. Energy* **2008**, *33*, 434–443. [[CrossRef](#)]
93. Zamora, B.; Kaiser, A.S. Numerical study on mixed buoyancy-wind driving induced flow in a solar chimney for building ventilation. *Renew. Energy* **2010**, *35*, 2080–2088. [[CrossRef](#)]
94. Neves, L.O.; Da Silva, F.M. Simulation and measurements of wind interference on a solar chimney performance. *J. Wind Eng. Ind. Aerodyn.* **2018**, *179*, 135–145. [[CrossRef](#)]
95. Shi, L. Impacts of wind on solar chimney performance in a building. *Energy* **2019**, *185*, 55–67. [[CrossRef](#)]
96. Wang, Q.; Zhang, G.; Li, W.; Shi, L. External wind on the optimum parameters of a wall solar chimney in building. *Sustain. Energy Technol. Assess.* **2020**, *42*, 100842. [[CrossRef](#)]
97. Moosavi, L.; Zandi, M.; Bidi, M.; Behroozzade, E.; Kazemi, I. New design for solar chimney with integrated windcatcher for space cooling and ventilation. *Build. Environ.* **2020**, *181*, 106785. [[CrossRef](#)]
98. Jomehzadeh, F.; Hussen, H.M.; Calaudit, J.K.; Nejat, P.; Ferwati, M.S. Natural ventilation by windcatcher (Bagdir): A review on the impacts of geometry, microclimate and macroclimate. *Energy Build.* **2020**, *226*, 110396. [[CrossRef](#)]
99. Evola, G.; Popov, V. Computational analysis of wind driven natural ventilation in buildings. *Energy Build.* **2006**, *38*, 491–501. [[CrossRef](#)]
100. Pakari, A.; Ghani, S. Aiflow assessment in a naturally ventilated greenhouse equipped with wind towers: Numerical simulation and wind tunnel experiments. *Energy Build.* **2019**, *199*, 1–11. [[CrossRef](#)]
101. Ramponi, R.; Blocken, B. CFD simulation of cross-ventilation for a generic isolated building: Impact of computational parameters. *Build. Environ.* **2012**, *53*, 34–48. [[CrossRef](#)]
102. Park, J.; Sun, X.; Choi, J.-I.; Rhee, G.H. Effect of wind and buoyancy interaction on single-sided ventilation in a building. *J. Wind Eng. Ind. Aerodyn.* **2017**, *171*, 380–389. [[CrossRef](#)]
103. Grimmond, C.S.B.; Oke, T.R. Aerodynamic properties of urban areas derived from analysis of surface form. *J. Appl. Meteorol.* **1999**, *38*, 1262–1292. [[CrossRef](#)]
104. Blocken, B.; Van der Hout, A.; Dekker, J.; Weiler, O. CFD simulation of wind flow over natural complex terrain: Case study with validation by field measurements for Ria de Ferrol, Galicia, Spain. *J. Wind Eng. Ind. Aerodyn.* **2015**, *147*, 43–57. [[CrossRef](#)]
105. Richards, P.J.; Hoxey, R.P. Appropriate boundary conditions for computational wind engineering models using the $k-\omega$ turbulence model. *J. Wind Eng. Ind. Aerodyn.* **1993**, *46–47*, 145–153. [[CrossRef](#)]
106. Blocken, B.; Stathopoulos, T.; Carmeliet, J. CFD simulations of the atmospheric boundary layer: Wall function problems. *Atmos. Environ.* **2007**, *41*, 238–252. [[CrossRef](#)]
107. Richards, P.J.; Norris, S.E. Appropriate boundary conditions for computational wind engineering models revised. *J. Wind Eng. Ind. Aerodyn.* **2011**, *99*, 257–266. [[CrossRef](#)]
108. Van Hoof, T.; Blocken, B.; Tominaga, Y. On the accuracy of CFD simulations of cross-ventilation flows for a generic isolated building: Comparison of RANS, LES and experiments. *Build. Environ.* **2017**, *114*, 148–165. [[CrossRef](#)]

109. Palyvos, J.A. A survey of wind convection coefficient correlations for building envelope energy systems' modeling. *Appl. Therm. Eng.* **2008**, *28*, 801–808. [[CrossRef](#)]
110. Zhang, H.; Yang, D.; Tam, V.W.Y.; Tao, Y.; Zhang, G.; Setunge, S.; Shi, L. A critical review of combined natural ventilation techniques in sustainable buildings. *Renew. Sustain. Energy Rev.* **2021**, *141*, 110795. [[CrossRef](#)]
111. Shaeri, J.; Mahdavejad, M. A new design to create natural ventilation in buildings: Wind chimney. *J. Build. Eng.* **2022**, *59*, 105041. [[CrossRef](#)]
112. Sakonidou, E.P.; Karapantsios, T.D.; Balouktis, A.I.; Chassapis, D. Modeling of the optimum tilt of a solar chimney for maximum air flow. *Sol. Energy* **2008**, *82*, 80–94. [[CrossRef](#)]
113. Prasad, M.; Chandra, K.S. Optimum tilt of solar collector for maximum natural flow. *Energy Convers. Manag.* **1990**, *30*, 369–379. [[CrossRef](#)]
114. Bassiouny, R.; Korah, N.S.A. Effect of solar chimney inclination angle on space flow pattern and ventilation rate. *Energy Build.* **2009**, *41*, 190–196. [[CrossRef](#)]
115. Khanal, R.; Lei, C. Flow reversal effects on buoyancy induced air flow in a solar chimney. *Sol. Energy* **2012**, *86*, 2783–2794. [[CrossRef](#)]
116. Khanal, R.; Lei, C. An experimental investigation of an inclined passive wall solar chimney for natural ventilation. *Sol. Energy* **2014**, *107*, 461–474. [[CrossRef](#)]
117. Ren, X.H.; Wang, L.; Liu, R.Z.; Wang, L.; Zhao, F.Y. Thermal stack airflows inside the solar chimney with discrete heat sources: Reversal flow regime defined by chimney inclination and thermal Rayleigh number. *Renew. Energy* **2021**, *163*, 342–356. [[CrossRef](#)]
118. Kong, J.; Niu, J.; Lei, C. A CFD based approach for determining the optimum inclination angle of a roof-top solar chimney for building ventilation. *Sol. Energy* **2020**, *198*, 555–569. [[CrossRef](#)]
119. Zavala-Guillén, I.; Xamán, J.; Hernández-Pérez, I.; Hernández-López, I.; Gijón-Rivera, M.; Chávez, Y. Numerical study of the optimum width of 2a diurnal double air-channel solar chimney. *Energy* **2018**, *47*, 403–417. [[CrossRef](#)]
120. Zamora, B. Morphological comparative assessment of a rooftop solar chimney through numerical modeling. *Int. J. Mech Sci.* **2022**, *227*, 107441. [[CrossRef](#)]
121. Al-Kayiem, H.H.; Sreejaya, K.V.; Ul-Haq Gilani, S.I. Mathematical analysis of the influence of the chimney height and collector area on the performance of a roof top solar chimney. *Energy Build.* **2014**, *68*, 305–311. [[CrossRef](#)]
122. Al-Kayiem, H.H.; Sreejaya, K.V.; Chikere, A.O. Experimental and numerical analysis of the influence of inlet configuration on the performance of a roof top solar chimney. *Energy Build.* **2018**, *159*, 89–98. [[CrossRef](#)]
123. He, G. A general model for predicting the airflow rates of a vertically installed solar chimney with connecting ducts. *Energy Build.* **2020**, *229*, 110481. [[CrossRef](#)]
124. He, G.; Zhang, J.; Hong, S. A new analytical model for airflow in solar chimneys based on thermal boundary layers. *Sol. Energy* **2016**, *136*, 614–621. [[CrossRef](#)]
125. Nguyen, Y.Q.; Wells, J.C. Effects of wall proximity on the airflow in a vertical solar chimney for natural ventilation of dwellings. *J. Build. Phys.* **2020**, *44*, 225–250. [[CrossRef](#)]
126. Nguyen, Y.Q.; Nguyen, V.T. Characterizing the induced flow through the cavity of a wall solar chimney under the effects of the opening heights. *J. Build. Phys.* **2022**. [[CrossRef](#)]
127. Fang, Z.; Wang, W.; Chen, Y.; Song, J. Structural and heat transfer model analysis of wall-mounted solar chimney inlets and outlets in single-story buildings. *Buildings* **2022**, *12*, 1790. [[CrossRef](#)]
128. Gao, N.; Yan, Y.; Sun, R.; Lei, Y. Natural ventilation enhancement of a roof solar chimney with wind-induced channel. *Energies* **2022**, *15*, 6492. [[CrossRef](#)]
129. Ren, X.H.; Liu, R.Z.; Wang, Y.H.; Wang, L.; Zhao, F.Y. Thermal driven natural convective flows inside the solar chimney flush-mounted with discrete heating sources: Reversal and cooperative flow dynamics. *Renew. Energy* **2019**, *138*, 354–367. [[CrossRef](#)]
130. Tkachenko, O.A.; Giroux-Julien, S.; Timchenko, V.; Ménézo, C.; Yeoh, G.H.; Reizes, J.A.; Sanvicente, E.; Fossa, M. Numerical and experimental investigation of unsteady natural convection in a non-uniformly heated vertical open-ended channel. *Int. J. Therm. Sci.* **2016**, *99*, 9–25. [[CrossRef](#)]
131. Zavala-Guillén, I.; Xamán, J.; Álvarez, G.; Arce, J.; Hernández-Pérez, I.; Gijón-Rivera, M. Computational fluid dynamics for modeling the turbulent natural convection in a double air-channel solar chimney system. *Int. J. Mod. Phys.* **2016**, *27*, 1650095. [[CrossRef](#)]
132. Zavala-Guillén, I.; Xamán, J.; Hernández-Pérez, I.; Hernández-López, I.; Jiménez-Xamán, C.; Moreno-Bernal, P.; Saucedo, D. Ventilation potential of an absorber-partitioned air channel solar chimney for diurnal use under Mexican climate conditions. *Appl. Therm. Eng.* **2019**, *149*, 807–821. [[CrossRef](#)]
133. He, G.; Lv, D. Distributed heat absorption in a solar chimney to enhance ventilation. *Sol. Energy* **2022**, *238*, 315–326. [[CrossRef](#)]
134. Lei, Y.; Zhang, Y.; Wang, F.; Wang, X. Enhancement of natural ventilation of a novel roof solar chimney with perforated absorber plate for building energy conservation. *Appl. Therm. Eng.* **2016**, *107*, 653–661. [[CrossRef](#)]
135. Chen, Z.D.; Bandopadhyay, P.; Halldorsson, J.; Byrjalsen, C.; Heiselberg, P.; Li, Y. An experimental investigation of a solar chimney model with uniform wall heat flux. *Build. Environ.* **2003**, *38*, 893–906. [[CrossRef](#)]
136. Wu, S.Y.; Yan, R.R.; Xiao, L. Numerically predicting the effect of fin on solar Trombe wall performance. *Sustain. Energy Technol. Assess.* **2022**, *52*, 102012. [[CrossRef](#)]

137. Hosseini, S.S.; Ramiar, A.; Ranjbar, A. Numerical investigation of rectangular fin geometry effect on solar chimney. *Energy Build.* **2017**, *155*, 296–307. [[CrossRef](#)]
138. Hosseini, S.S.; Ramiar, A.; Ranjbar, A. Numerical investigation of natural convection solar air heater with different fins shape. *Renew. Energy* **2018**, *117*, 488–500. [[CrossRef](#)]
139. Promvong, P.; Promthaisong, P.; Skullong, S. Numerical heat transfer in a solar air heater duct with punched delta-winglet vortex generators. *Case Stud. Therm. Eng.* **2021**, *26*, 101088. [[CrossRef](#)]
140. Jin, D.; Quan, S.; Zuo, J.; Xu, S. Numerical investigation of heat transfer enhancement in a solar air heater roughened by multiple V-shaped ribs. *Renew. Energy* **2019**, *134*, 78–88. [[CrossRef](#)]
141. Arunkumar, H.S.; Kumar, S.; Karanth, K.V. Analysis of a solar air heater for augmented thermohydraulic performance using helicoidal spring shaped fins—A numerical study. *Renew. Energy* **2020**, *160*, 297–311. [[CrossRef](#)]
142. Shi, J.; Hu, J.; Schafer, S.R.; Chen, C.L. Numerical study of heat transfer enhancement of channel via vortex-induced vibration. *Appl. Therm. Eng.* **2014**, *70*, 838–845. [[CrossRef](#)]
143. Nguyen, Y.Q.; Huynh, T.N.; Pham, M.-A.H. Modifications of heat transfer and induced flow rate of a solar chimney by an obstacle in the air channel. *Int. J. Adv. Sci. Eng. Inf. Technol.* **2021**, *11*, 482–488. [[CrossRef](#)]
144. Gandjalikhan Nassab, S.A.; Sheikhnajad, Y.; Foruzan Nia, M. Novel design of natural solar air heat for higher thermal performance. *Therm. Sci. Eng. Prog.* **2022**, *33*, 101385. [[CrossRef](#)]
145. Sheikhnajad, Y.; Gandjalikhan Nassab, S.A. Enhancement of solar chimney performance by passive vortex generator. *Renew. Energy* **2021**, *169*, 437–450. [[CrossRef](#)]
146. Monghasemi, N.; Vadiiee, A. A review of solar chimney integrated systems for space heating and cooling application. *Renew. Sustain. Energy Rev.* **2018**, *81*, 2714–2730. [[CrossRef](#)]
147. Maghrabie, H.M.; Abdelkareem, M.A.; Elsaid, K.; Sayed, E.T.; Radwan, A.; Rezk, H.; Wilberforce, T.; Abo-Khalil, A.G.; Olabi, A.G. A review of solar chimney for natural ventilation of residential and non-residential building. *Sustain. Energy Technol. Assess.* **2022**, *52*, 102082. [[CrossRef](#)]
148. Miyazaki, T.; Akisawa, A.; Kashiwagi, T. The effects of solar chimneys on thermal load mitigation of office buildings under the Japanese climate. *Renew. Energy* **2006**, *31*, 987–1010. [[CrossRef](#)]
149. Chugloo, S.; Limmeechokchai, B. Application of passive cooling system in the hot and humid climate: The case study of solar chimney and wetted roof in Thailand. *Build. Environ.* **2007**, *42*, 3341–3351. [[CrossRef](#)]
150. Abdallah, A.S.H.; Hiroshi, Y.; Goto, T.; Enteria, N.; Radwan, M.M.; Eid, M.A. Parametric investigation of solar chimney with new cooling tower integrated in a single room for New Assiut city, Egypt climate. *Int. J. Energy Environ. Eng.* **2014**, *5*, 1–9. [[CrossRef](#)]
151. Sudpraset, S.; Chinsorranant, C.; Rattanedcho, P. Numerical study of vertical chimneys with moist air in a hot and humid climate. *Int. J. Heat Mass Transf.* **2016**, *102*, 645–656. [[CrossRef](#)]
152. Yusoff, W.F.M.; Salleh, E.; Adam, N.M.; Sapian, A.R.; Sulaiman, M.Y. Enhancement of stack ventilation in hot and humid climate using a combination of roof solar collector and vertical stack. *Build. Environ.* **2010**, *45*, 2296–2308. [[CrossRef](#)]
153. Zhu, N.; Li, S.; Hu, P.; Lei, F.; Deng, R. Numerical investigations on performance of phase change material Trombe wall in building. *Energy* **2019**, *187*, 116057. [[CrossRef](#)]

Disclaimer/Publisher’s Note: The statements, opinions and data contained in all publications are solely those of the individual author(s) and contributor(s) and not of MDPI and/or the editor(s). MDPI and/or the editor(s) disclaim responsibility for any injury to people or property resulting from any ideas, methods, instructions or products referred to in the content.